NASA TECHNICAL MEMORANDUM

NASA TM X-1620

NASA TM X-1620

HYPERSONIC AERODYNAMIC CHARACTERISTICS OF LOW-WAVE-DRAG ELLIPTICAL-BODY–TAIL COMBINATIONS AS AFFECTED BY CHANGES IN STABILIZER CONFIGURATION

by Charles H. Fox, Jr., and Bernard Spencer, Jr.

Langley Research Center

Langley Station, Hampton, Va.

NATIONAL AERONAUTICS AND SPACE ADMINISTRATION • WASHINGTON, D. C. • AUGUST 1968

NASA TM X-1620

HYPERSONIC AERODYNAMIC CHARACTERISTICS OF LOW-WAVE-DRAG ELLIPTICAL-BODY—TAIL COMBINATIONS AS AFFECTED BY CHANGES IN STABILIZER CONFIGURATION

By Charles H. Fox, Jr., and Bernard Spencer, Jr.

Langley Research Center
Langley Station, Hampton, Va.

NATIONAL AERONAUTICS AND SPACE ADMINISTRATION

For sale by the Clearinghouse for Federal Scientific and Technical Information
Springfield, Virginia 22151 – CFSTI price $3.00

HYPERSONIC AERODYNAMIC CHARACTERISTICS OF LOW-WAVE-DRAG ELLIPTICAL-BODY—TAIL COMBINATIONS AS AFFECTED BY CHANGES IN STABILIZER CONFIGURATION

By Charles H. Fox, Jr., and Bernard Spencer, Jr.
Langley Research Center

SUMMARY

An investigation has been made in the Langley 15-inch hypersonic flow apparatus at a Mach number of 10.03 in air to determine systematically the effects of outboard stabilizer and vertical- and vee-tail configurations on the longitudinal- and lateral-directional stability characteristics and on the resultant aerodynamic performance of a low-wave-drag elliptical body. The body had a longitudinal area distribution conforming to the theoretical shape required to minimize the zero-lift hypersonic pressure drag under the constraints of given length and volume. The body cross section was elliptical with a major-to-minor axis ratio of 2 (major axis horizontal). Bodies were tested with equivalent fineness ratios of 6.14 and 9.83. Base-mounted outboard stabilizers were tested at various dihedral angles alone and in combination with either a single center-line vertical tail or with a vee tail. The angle of attack was varied from approximately -4° to 21° at 0° and -5° of sideslip. This investigation represents the initial portion of a study to determine methods of providing stability from hypersonic through low subsonic speeds for vehicles with high hypersonic lift-drag ratios.

The results of this investigation indicate that the maximum untrimmed lift-drag ratio is reduced approximately 15 percent due to the outboard stabilizers for either fineness-ratio body. The resultant aerodynamic performance is, however, relatively insensitive to changes in the outboard stabilizer dihedral angle for any given configuration tested. For a moment reference location selected as 55 percent of the body length, the outboard stabilizers set at positive dihedral angles provide positive pitching moment at zero angle of attack, less out-of-trim pitching moment at maximum lift-drag ratio, and resultantly less increase in stability variation with increasing angle of attack as compared with outboard stabilizers set at negative dihedral angles. In addition, the directional-stability parameter at maximum lift-drag ratio varies nonlinearly with outboard stabilizer dihedral angle with a maximum stabilizing effect indicated in the dihedral-angle region from 30° to 60° for positive dihedrals.

INTRODUCTION

Numerous experimental investigations have been performed recently to examine methods of improving the hypersonic aerodynamic performance of a certain class of lifting bodies having variations in both longitudinal contour and cross-sectional shape. Results of parametric studies, such as references 1 and 2, have indicated that bodies designed to minimize pressure drag at hypersonic speeds can provide significant improvements in aerodynamic performance as compared, for example, with conical bodies. Since these body shapes were envisioned for such uses as high-performance entry vehicles or as components of hypersonic cruise vehicles, they were systematically studied from hypersonic through low subsonic speeds, that is, in the speed range in which the vehicles would operate. (See refs. 3 and 4.) The studies reported in references 1 to 4 are primarily concerned with the aerodynamic performance of lifting bodies and no attempt was made to examine methods of stabilizing the bodies.

Therefore, a systematic study has been initiated to examine methods of providing stability for a particular member of the family of bodies in references 1 to 4. The present investigation was made in the Langley 15-inch hypersonic flow apparatus to provide generalized information on the effects of outboard stabilizer and vertical- and vee-tail configurations on the overall aerodynamic characteristics of a particular lifting-body configuration at hypersonic speeds. Two bodies were tested which had equivalent fineness ratios of 6.14 and 9.83. These bodies were elliptical in cross section with a major-to-minor axis ratio of 2 (major axis horizontal). The longitudinal contours were designed to conform to the theoretical shape required to minimize the zero-lift pressure drag at hypersonic speeds for the geometric constraints of given length and volume (ref. 1). Base-mounted outboard stabilizers were tested at various dihedral angles alone and in combination with either a single center-line vertical tail or with a vee tail. Tests were made at a Mach number of 10.03 in air. The angle-of-attack range was from approximately -4° to 21° at 0° and -5° of sideslip.

SYMBOLS

Longitudinal data are presented about the stability axes and lateral-directional data are presented about the body axes. All coefficients are normalized with respect to the projected planform area, length, and span of the particular body. The longitudinal moment reference point was selected as 55 percent of the body length for each configuration with the vertical moment reference point on the body center line.

a semimajor axis of ellipse (semispan of body), feet (meters)

A_b base area of body, feet^2 (meters^2)

b semiminor axis of ellipse (one-half the base height of body), feet (meters)

C_D drag coefficient, $\frac{\text{Drag}}{qS}$

$C_{D,min}$ minimum drag coefficient

C_L lift coefficient, $\frac{\text{Lift}}{qS}$

C_{L_α} lift-curve slope, $\frac{\partial C_L}{\partial \alpha}$ at $\alpha \approx 0^o$, per degree

C_l rolling-moment coefficient, $\frac{\text{Rolling moment}}{2aqS}$

C_{l_β} lateral-stability parameter, $\frac{\Delta C_l}{\Delta \beta}$ at $\beta \approx 0^o$ and -5^o, per degree

C_m pitching-moment coefficient, $\frac{\text{Pitching moment}}{qSl}$

$C_{m,o}$ pitching-moment coefficient at $\alpha = 0^o$

C_N normal-force coefficient, $\frac{\text{Normal force}}{qS}$

C_n yawing-moment coefficient, $\frac{\text{Yawing moment}}{2aqS}$

C_{n_β} directional-stability parameter, $\frac{\Delta C_n}{\Delta \beta}$ at $\beta \approx 0^o$ and -5^o, per degree

C_Y side-force coefficient, $\frac{\text{Side force}}{qS}$

C_{Y_β} side-force parameter, $\frac{\Delta C_Y}{\Delta \beta}$ at $\beta \approx 0^o$ and -5^o, per degree

f equivalent fineness ratio, $\frac{l}{2\sqrt{ab}}$

l length of body, feet (meters)

L/D lift-drag ratio

$(L/D)_{max}$ maximum lift-drag ratio

q free-stream dynamic pressure, pounds/square foot (newtons/meter^2)

R Reynolds number based on body length

S projected planform area of body, feet^2 (meters^2)

S_t exposed planform area of stabilizer or tail, feet^2 (meters^2)

S_{wet} wetted area of body, feet^2 (meters^2)

x_{cp}/l center-of-pressure location in percent body length ($\alpha \approx 0^o$), $\frac{x_{cp}}{l} = 0.55 - \frac{\partial C_m}{\partial C_N}$

α angle of attack, degrees

β angle of sideslip, degrees

Γ_s stabilizer dihedral angle; the axis of rotation is a line parallel to the body longitudinal axis and passing through the semi-major axis at the point defined as the semispan of the body minus one-half of the root base thickness of the stabilizer (fig. 1)

θ_v tail dihedral angle; the axis of rotation is the body longitudinal axis (fig. 1)

Subscript:

$(L/D)_{max}$ conditions at maximum lift-drag ratio

MODELS

The models used in the present investigation had equivalent fineness ratios of 6.14 and 9.83. The models were elliptical minimum-wave-drag bodies (volume and length constraints) with the major-to-minor axis ratio equal to 2 and the major axis horizontal. Details of the models are presented in figure 1 and photographs of the models are presented in figure 2.

For either body fineness ratio, the configurations tested were as follows:

(a) Body alone.

(b) Body in combination with outboard stabilizers in the dihedral range from -90^o to 90^o.

(c) Body in combination with single center-line vertical tail ($\theta_v = 90^o$) and the outboard stabilizers in the dihedral range from -90^o to 90^o.

(d) Body in combination with vee tail ($\theta_v = 30^o$) and outboard stabilizers in the dihedral range from -90^o to 0^o.

The longitudinal contours of the bodies were designed to have minimum zero-lift hypersonic pressure drag under the constraints of given length and volume (ref. 1). The pertinent geometric constants are given in table I. Slight differences exist between the actual tail and stabilizer dimensions and the nominal dimensions; therefore, the dimensions given in figures 1(b) and 1(d) represent actual measurements. The ratio of the exposed area of a given tail or set of tails or set of stabilizers to the reference area is also presented in table I.

TABLE I.- GEOMETRIC CONSTANTS

f	l	$\frac{S}{l^2}$	$\frac{S_{wet}}{l^2}$	$\frac{A_b}{l^2}$	$\frac{S_t}{S}$		$\frac{S_t}{S}$
					$\theta_v = 90^o$	$\theta_v = 30^o$	(Γ_s any value)
6.14	1 ft (0.3048 m)	0.1504	0.362	0.0208	0.0737	0.147	0.146
9.83	1.1666 ft (0.3556 m)	0.1010	0.229	0.00813	0.0735	0.147	0.150

APPARATUS, TESTS, AND CORRECTIONS

The present investigation was made in the Langley 15-inch hypersonic flow apparatus at a Mach number of 10.03 in air. Forces and moments were measured with a sting-supported, internally mounted, water-cooled, six-component strain-gage balance. A brief description of this facility is given in reference 3.

Tests were made at a stagnation temperature of 1100^o F (593.3^o C) and a stagnation pressure of approximately 800 lb/in^2 (5516 kN/m^2) corresponding to free-stream Reynolds numbers based on body length R of 1.488×10^6 and 1.736×10^6 for the fineness ratio 6.14 and 9.83 bodies, respectively. The angle-of-attack range was from approximately -4^o to 21^o at 0^o and -5^o of sideslip. The angle of attack has been corrected for sting and balance deflections under load. Base-pressure measurements were not taken and therefore the drag data are all uncorrected for the effects of base pressure.

The lateral- and directional-stability parameters C_{l_β}, C_{n_β}, and C_{Y_β} have been computed from data obtained at sideslip angles of 0^o and -5^o. It has been assumed that the variation of C_l, C_n, and C_Y with sideslip angle is linear between $\beta = 0^o$ and -5^o for all configurations tested throughout the angle-of-attack range from approximately -4^o to 21^o.

PRESENTATION OF RESULTS

The basic data for the configurations tested in the present study are presented in figures 3 to 18. Longitudinal characteristics are presented in part (a) and lateral-directional characteristics are presented in part (b) of each figure. The following table is presented as an aid in locating a particular set of experimental results:

DISCUSSION OF RESULTS

Effect of Tails

The basic body possesses a maximum lift-drag ratio of approximately 3.46 for the $f = 6.14$ body and 3.62 for the $f = 9.83$ body. The addition of a single center-line vertical tail $(\theta_v = 90^o)$ results in a small reduction in $(L/D)_{max}$ to 3.32 and 3.34 for the $f = 6.14$ and 9.83 bodies, respectively. However, the addition of a vee tail $(\theta_v = 30^o)$ to

the basic body results in a large loss in untrimmed $(L/D)_{max}$ to 2.70 for the $f = 6.14$ body and to 3.07 for the $f = 9.83$ body. (See figs. 3(a) and 9(a).) As would be expected, the vee tails $(\theta_v = 30^o)$ also considerably increase the stability of the configurations.

The addition of either the center-line vertical tail or the vee tail increased the directional stability for either fineness-ratio body tested (figs. 3(b) and 9(b)), the largest increase occurring from addition of the vee tail. Increases in positive effective dihedral $\left(-C_{l_\beta}\right)$ were also noted with the addition of the tails.

Effect of Outboard Stabilizers

The addition of outboard stabilizers (at $\Gamma_s = 0^o$) to the configurations with either the center-line tail or the vee tail further reduced the performance (figs. 3(a) and 9(a)) due to large increases in $C_{D,min}$. However, the body with the center-line tail and outboard stabilizers at $\Gamma_s = 0^o$ was superior in performance compared with the body with vee tail and outboard stabilizers at $\Gamma_s = 0^o$ because of the lower drag associated with the smaller tail-surface area.

The addition of outboard stabilizers at $\Gamma_s = 0^o$ to either fineness-ratio-body—tail configuration further increased both the lateral and the directional stability. (See figs. 3(b) and 9(b).) The body with the vee tail and outboard stabilizers at $\Gamma_s = 0^o$ exhibited better lateral and directional stability characteristics when compared with the corresponding configuration having the center-line vertical tail.

Effect of Stabilizer Dihedral

Varying the dihedral angle of the basic outboard stabilizers produced only slight changes in the resultant $(L/D)_{max}$ for either fineness-ratio body (figs. 15 and 16). In general, increasing the stabilizer dihedral angle produced a more positive $C_{m,o}$, less out-of-trim moment near $(L/D)_{max}$, and resultantly less increase in longitudinal stability variation with increasing α, when compared with the negative dihedral stabilizer. (See figs. 4(a), 5(a), 10(a), and 11(a).)

Configurations with the outboard stabilizers set at positive dihedral angles exhibited better directional stability characteristics throughout the test angle-of-attack range when compared with configurations with the outboard stabilizers set at negative dihedral angles. (Compare figs. 4(a) and 5(b) ($f = 6.14$) and figs. 10(b) and 11(b) ($f = 9.83$).) As would be expected, higher values of positive effective dihedral $\left(-C_{l_\beta}\right)$ resulted from use of the outboard stabilizers at positive dihedral angles.

Summary of Characteristics at $(L/D)_{max}$

A summary of the $(L/D)_{max}$ and C_m at $(L/D)_{max}$ characteristics is presented in figures 15 and 16 for the $f = 6.14$ and 9.83 bodies, respectively. The values of C_m at $(L/D)_{max}$ are presented to point out that the $(L/D)_{max}$ values shown are, in general, for an untrimmed condition.

As the dihedral angle of the outboard stabilizers Γ_s is increased from -90^o to 90^o, the maximum out-of-trim moment (i.e., C_m at $(L/D)_{max}$) occurs in the region from $\Gamma_s = -60^o$ to -30^o. As Γ_s increases beyond that point, the out-of-trim moment (i.e., C_m at $(L/D)_{max}$) decreases until the configuration with $\Gamma_s = 90^o$ is almost trimmed. The pitching moments are presented about the selected moment reference point. The lower out-of-trim moment at positive values of Γ_s would result in a much lower trim drag penalty compared with corresponding negative values of Γ_s. As previously noted, the configuration with outboard stabilizers at positive values of Γ_s possesses positive values of $C_{m,o}$ and is less stable than the configuration with corresponding negative values of Γ_s.

A summary of the lateral-directional stability characteristics at $(L/D)_{max}$ is presented in figures 17 and 18 for the $f = 6.14$ and 9.83 bodies, respectively. All configurations tested except the body alone possess directional stability at $(L/D)_{max}$, and all configurations indicate lateral stability except for the $f = 9.83$ body with $\Gamma_s = -90^o$ and θ_v = Off and 90^o. However, the directional-stability parameter at $(L/D)_{max}$ varies nonlinearly with Γ_s with a maximum value occurring for positive dihedrals in the region from $\Gamma_s = 30^o$ to 60^o for either fineness-ratio body. For negative outboard stabilizer dihedrals, increasing negative dihedral from $\Gamma_s = 0^o$ to -90^o increases C_{n_β} at $(L/D)_{max}$ except in the region of $\Gamma_s = -30^o$ for either fineness-ratio body. A comparison of $\pm\Gamma_s$ indicates that maximum C_{n_β} at $(L/D)_{max}$ occurs at $\Gamma_s = 30^o$ $(\theta_v$ = Off, $90^o)$ for the $f = 6.14$ body and at $\Gamma_s = -90^o$ $(\theta_v$ = Off, $90^o)$ for the $f = 9.83$ body. It is of interest to note the loss in C_{n_β} as Γ_s increases from 60^o to 90^o, an indication that the loss in stabilizing effectiveness might be due to a partial shadowing of the stabilizing surface.

CONCLUDING REMARKS

An investigation has been made in the Langley 15-inch hypersonic flow apparatus at a Mach number of 10.03 in air to determine systematically the effects of outboard stabilizer and vertical- and vee-tail configurations on the longitudinal- and lateral-directional stability characteristics and on the resultant aerodynamic performance of low-wave-drag elliptical bodies having equivalent fineness ratios of 6.14 and 9.83. This investigation represents the initial portion of a study to determine methods of providing stability for vehicles with high hypersonic lift-drag ratios from hypersonic through subsonic speeds.

The results of this investigation indicate that the maximum untrimmed lift-drag ratio is reduced approximately 15 percent due to the outboard stabilizers for either fineness-ratio body. The resultant aerodynamic performance is, however, relatively insensitive to changes in the outboard stabilizer dihedral for any given configuration tested. For a moment reference location selected as 55 percent of the body length, the outboard stabilizers set at positive dihedral angles provide positive pitching moment at zero angle of attack, less out-of-trim pitching moment at maximum lift-drag ratio, and resultantly less increase in stability variation with increasing angle of attack as compared with outboard stabilizers set at negative dihedral angles. In addition, the directional-stability parameter at maximum lift-drag ratio varies nonlinearly with outboard stabilizer dihedral angle with a maximum stabilizing effect indicated in the dihedral-angle region from 30° to 60° for positive dihedrals.

Langley Research Center,
National Aeronautics and Space Administration,
Langley Station, Hampton, Va., April 19, 1968,
124-07-02-01-23.

REFERENCES

1. Spencer, Bernard, Jr.; and Fox, Charles H., Jr.: Hypersonic Aerodynamic Performance of Minimum-Wave-Drag Bodies. NASA TR R-250, 1966.

2. Spencer, Bernard, Jr.: Hypersonic Aerodynamic Characteristics of Minimum-Wave-Drag Bodies Having Variations in Cross-Sectional Shape. NASA TN D-4079, 1967.

3. Spencer, Bernard, Jr.: Transonic Aerodynamic Characteristics of a Series of Related Bodies With Cross-Sectional Ellipticity. NASA TN D-3203, 1966.

4. Fournier, Roger H.; Spencer, Bernard, Jr.; and Corlett, William A.: Supersonic Aerodynamic Characteristics of a Series of Related Bodies With Cross-Sectional Ellipticity. NASA TN D-3539, 1966.

5. Putnam, Lawrence E.; and Brooks, Cuyler W., Jr.: Static Longitudinal Aerodynamic Characteristics at a Mach Number of 10.03 of Low-Aspect-Ratio Wing-Body Configurations Suitable for Reentry. NASA TM X-733, 1962.

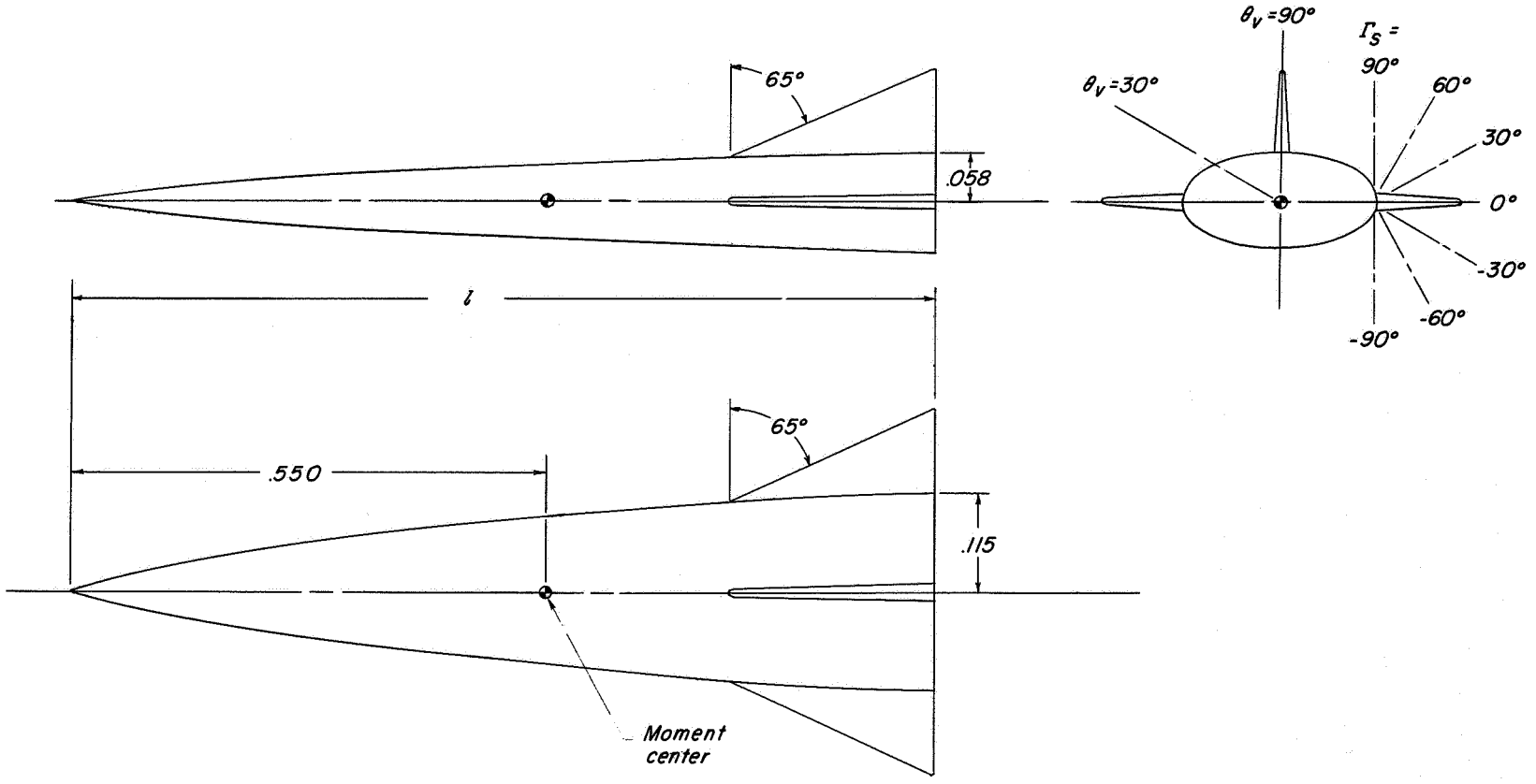

(a) General arrangement of f = 6.14 body. l = 1 ft (0.3048 m).

Figure 1.- Details of the elliptical low-wave-drag bodies tested, including outboard stabilizer and vertical- and vee-tail locations. The dimensions for the center-line vertical tail, vee-tail, and stabilizers are the same for all configurations. (All linear dimensions are nondimensionalized with respect to body length.)

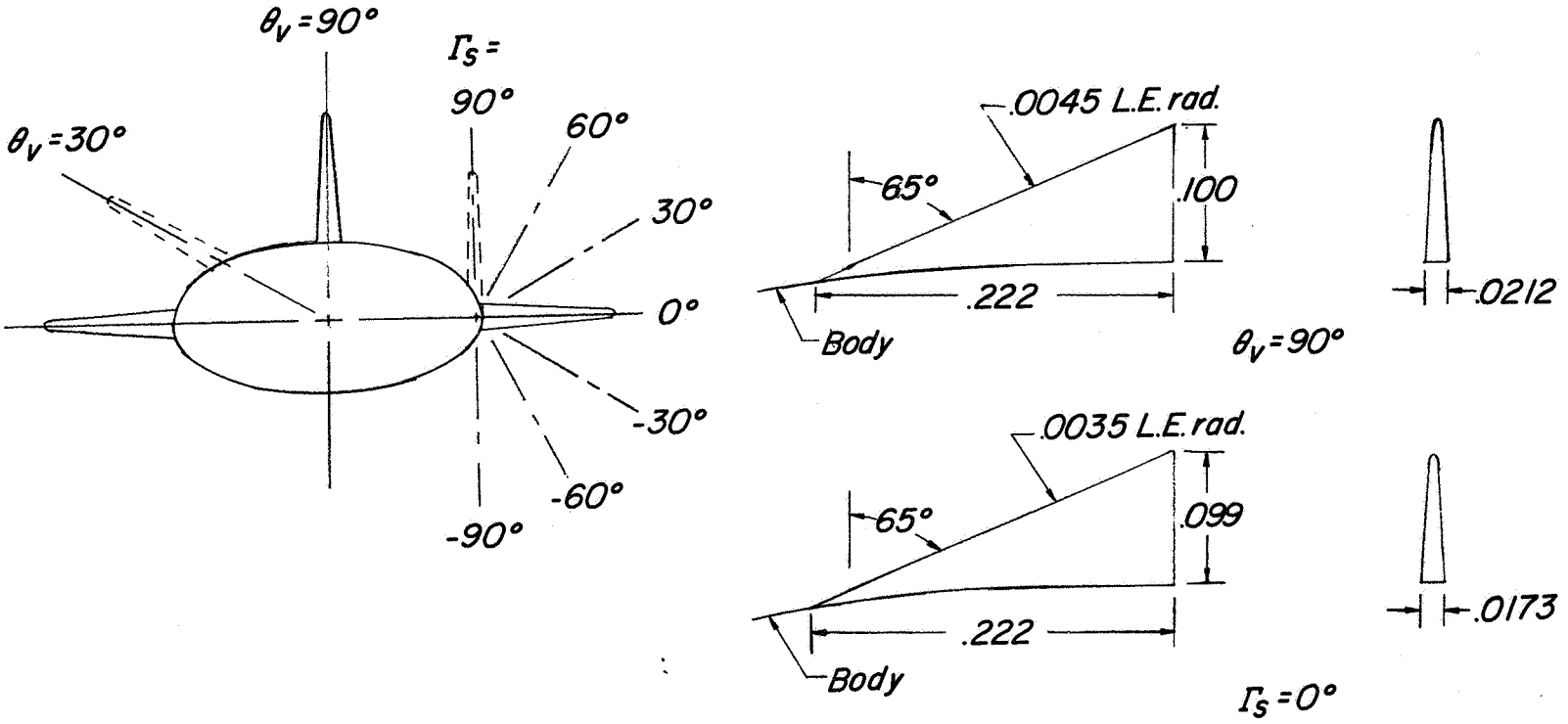

(b) Tail and stabilizer configurations of f = 6.14 body. ℓ = 1 ft (0.3048 m).

Figure 1.- Continued.

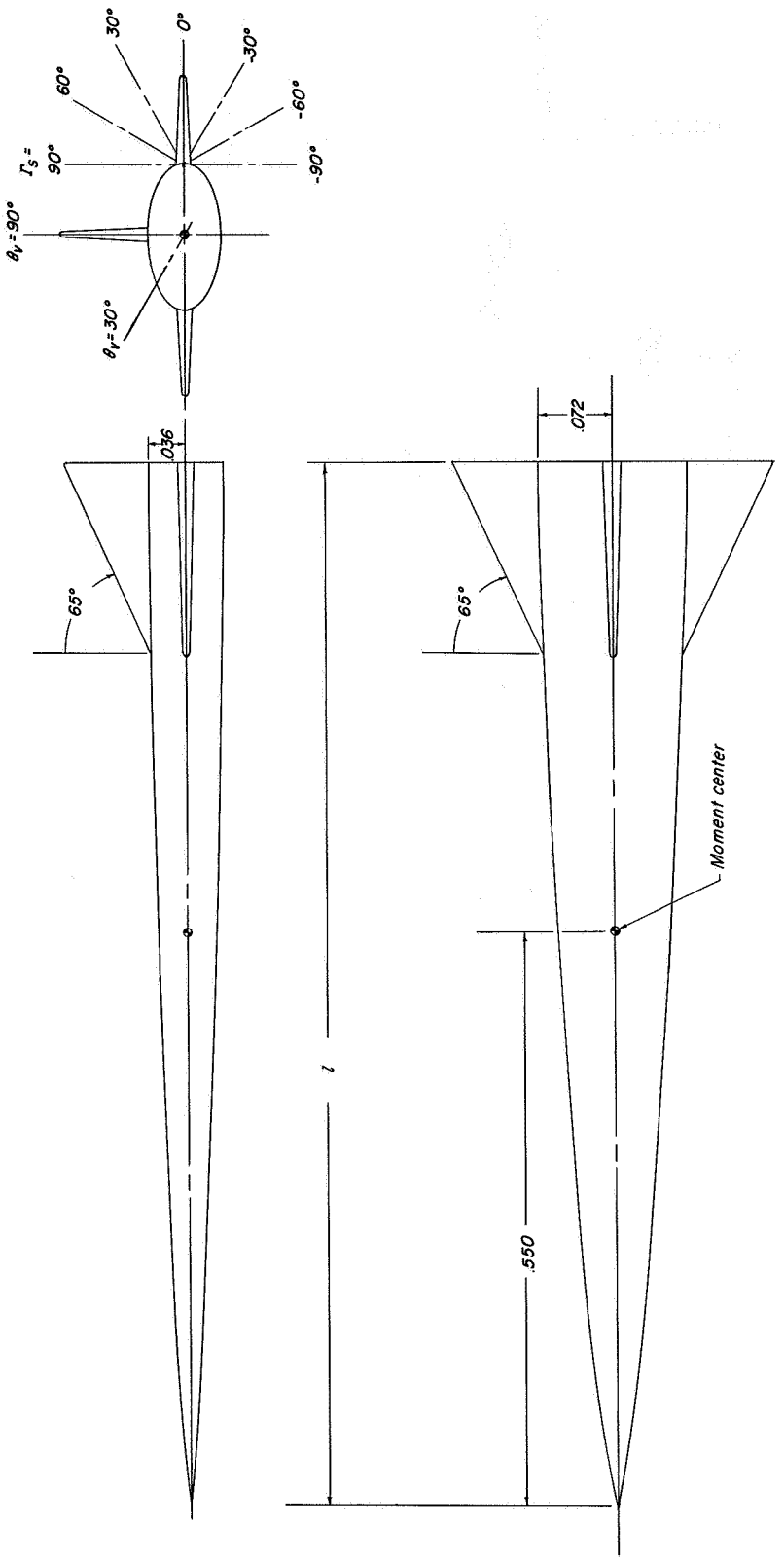

(c) General arrangement of f = 9.83 body. l = 1.1666 ft (0.3556 m).

Figure 1.- Continued.

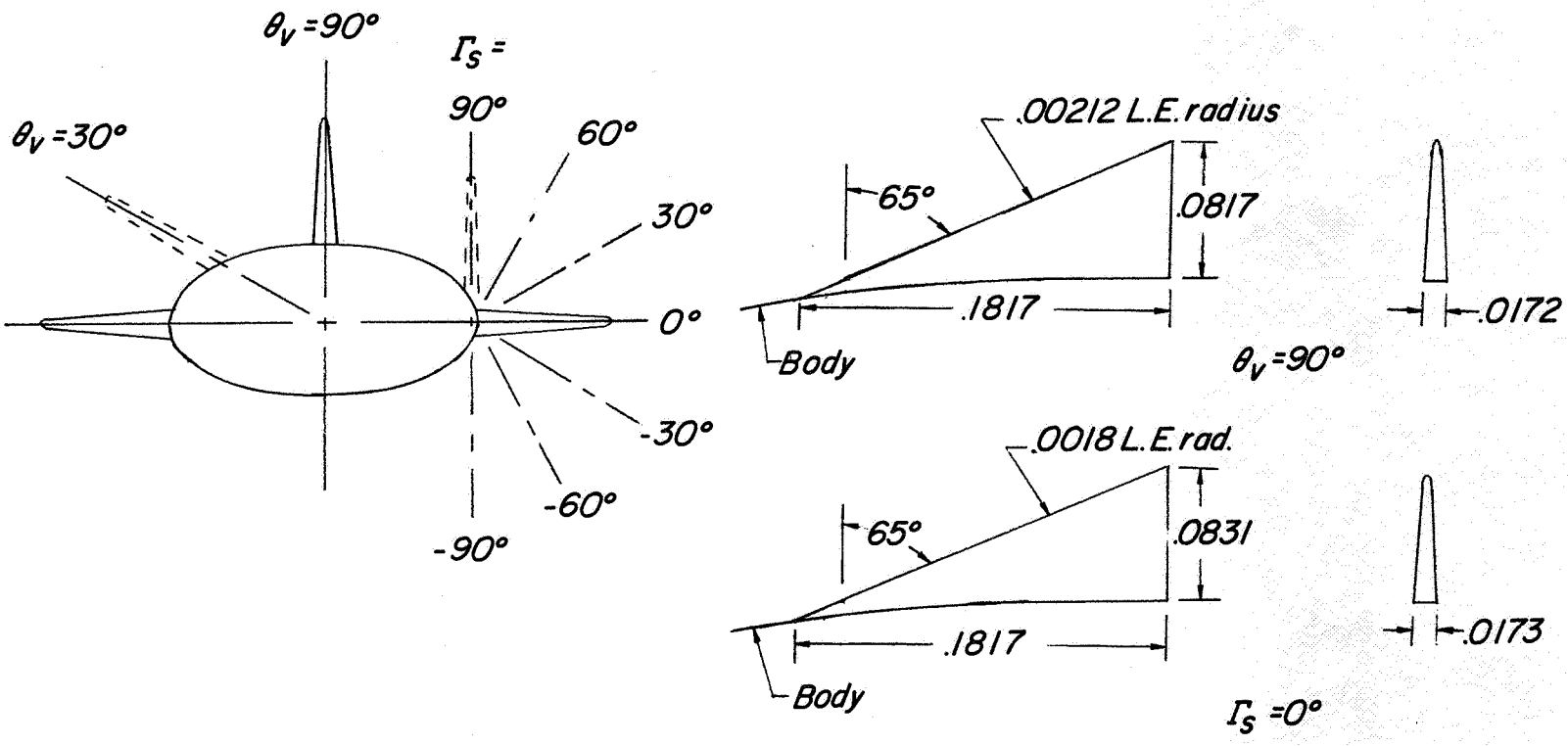

(d) Tail and stabilizer configurations of f = 9.83 body. ℓ = 1.1666 ft (0.3556 m).

Figure 1.- Concluded.

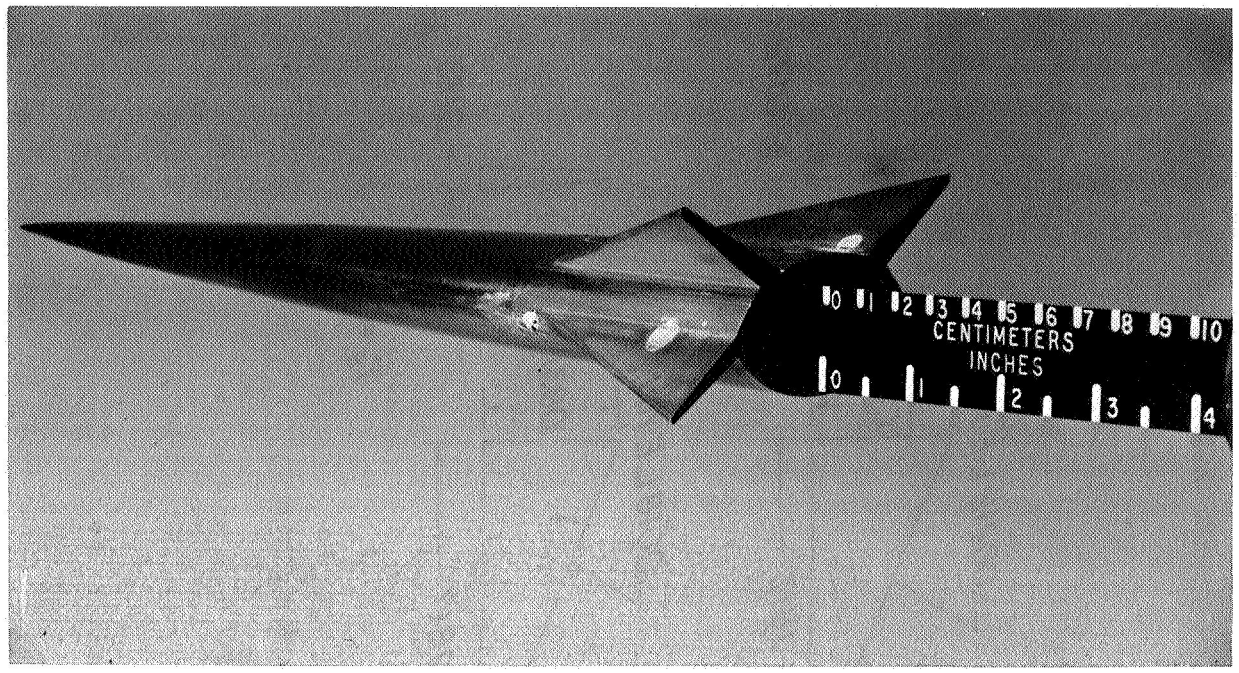

(a) The f = 6.14 body with $\theta_v = 30^0$ and $\Gamma_s = -30^0$. L-67-1542

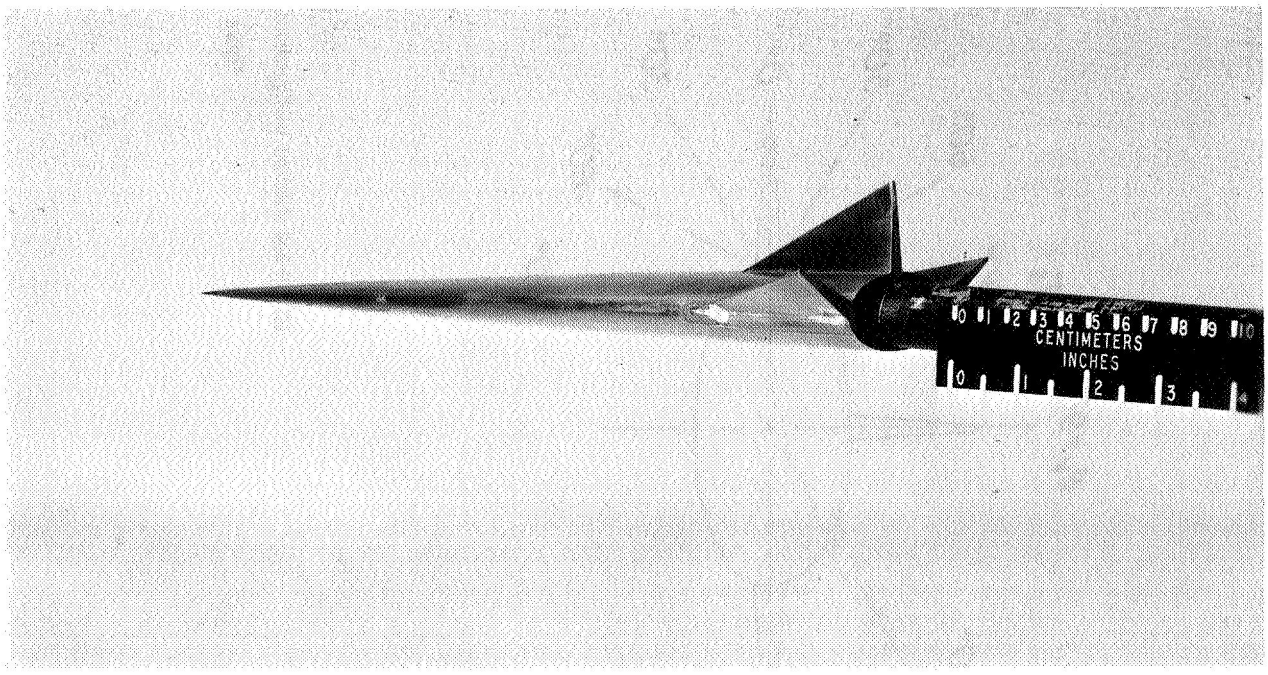

(b) The f = 9.83 body with $\theta_v = 90^0$ and $\Gamma_s = 30^0$. L-67-1543

Figure 2.- Models used in the investigation.

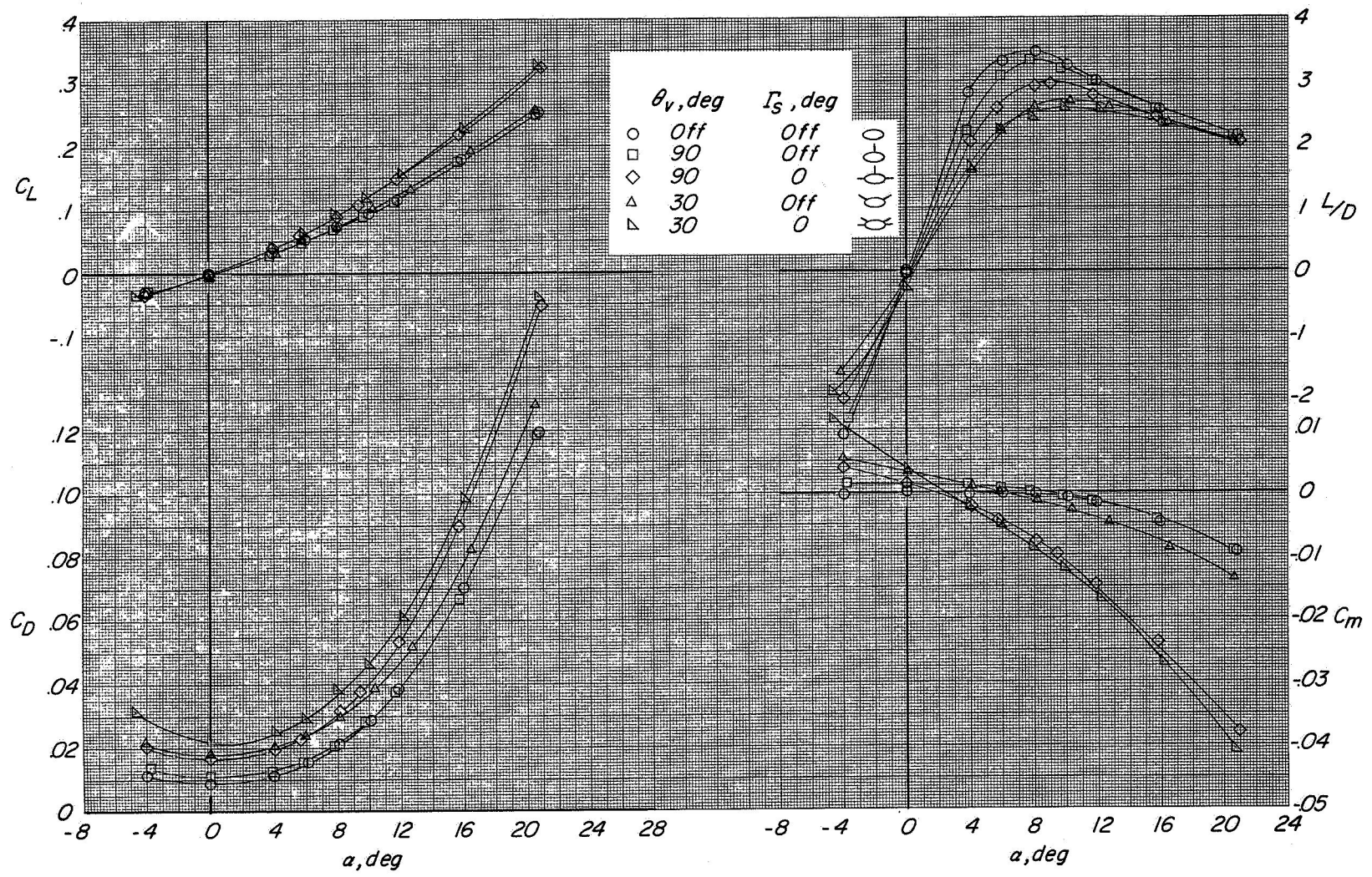

(a) Longitudinal characteristics.

Figure 3.- Effect of addition of tails and stabilizers on aerodynamic characteristics of f = 6.14 body.

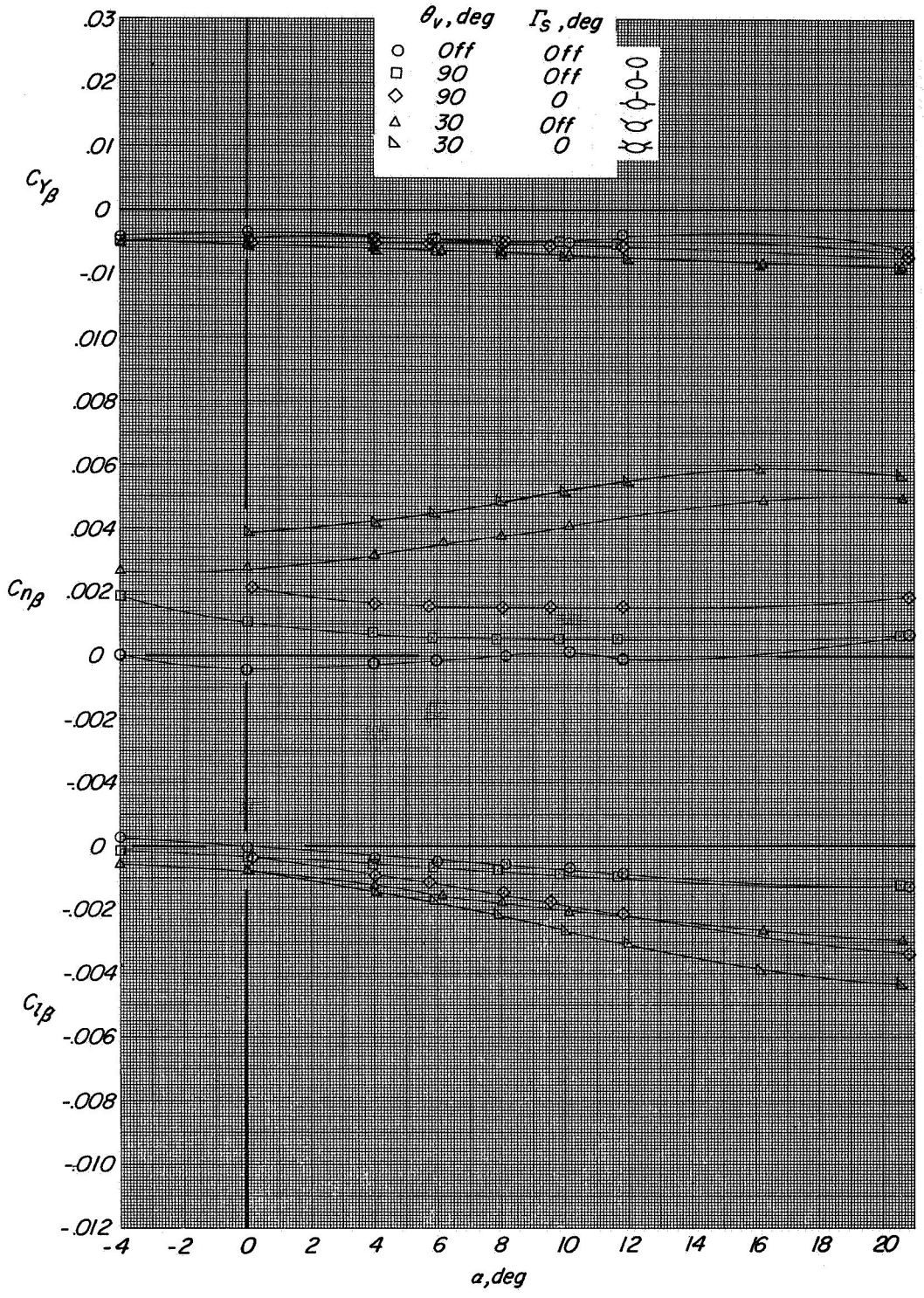

(b) Lateral-directional characteristics.

Figure 3.- Concluded.

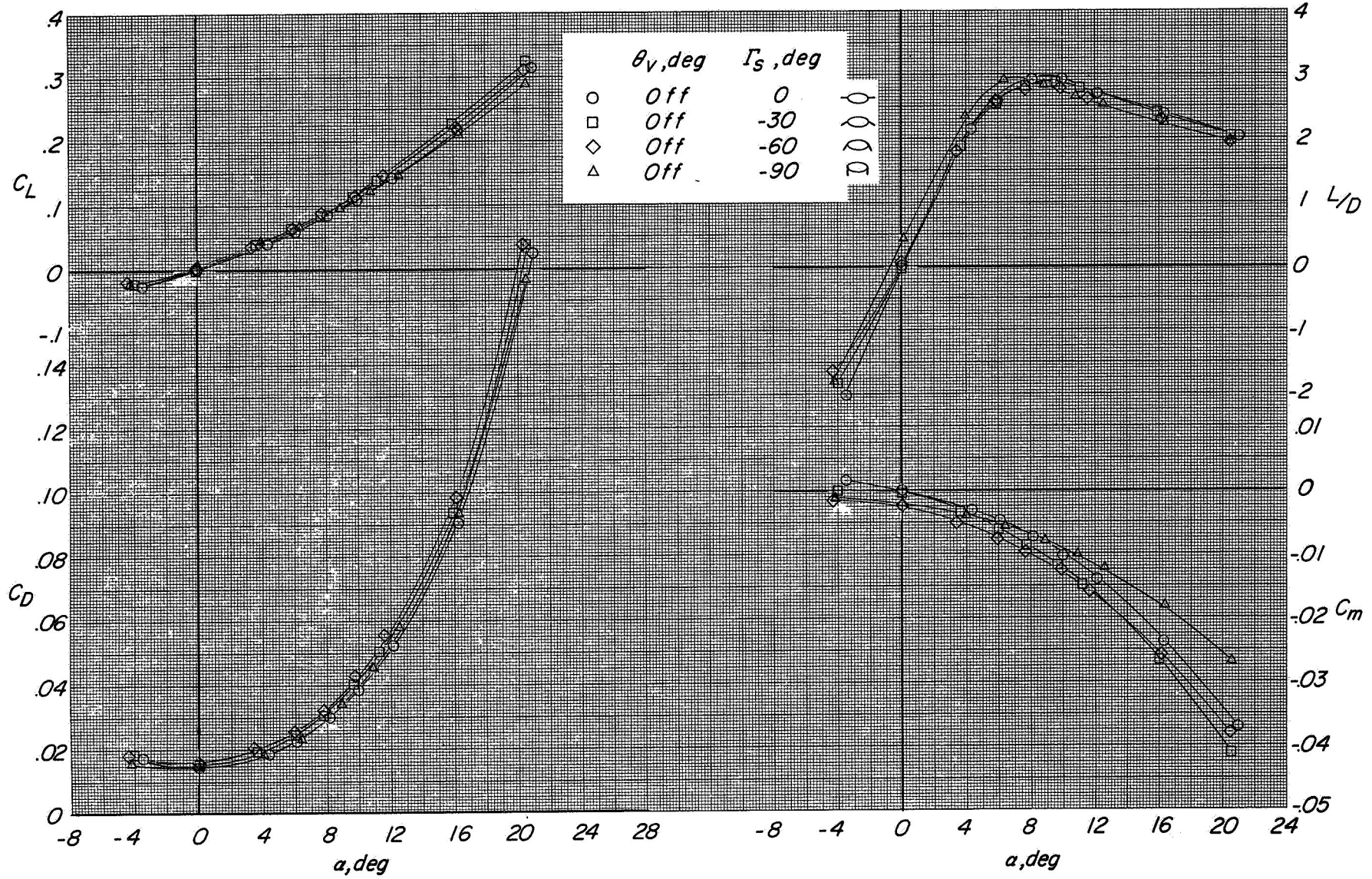

(a) Longitudinal characteristics.

Figure 4.- Effect of outboard stabilizers at negative dihedral angles on aerodynamic characteristics of f = 6.14 body.

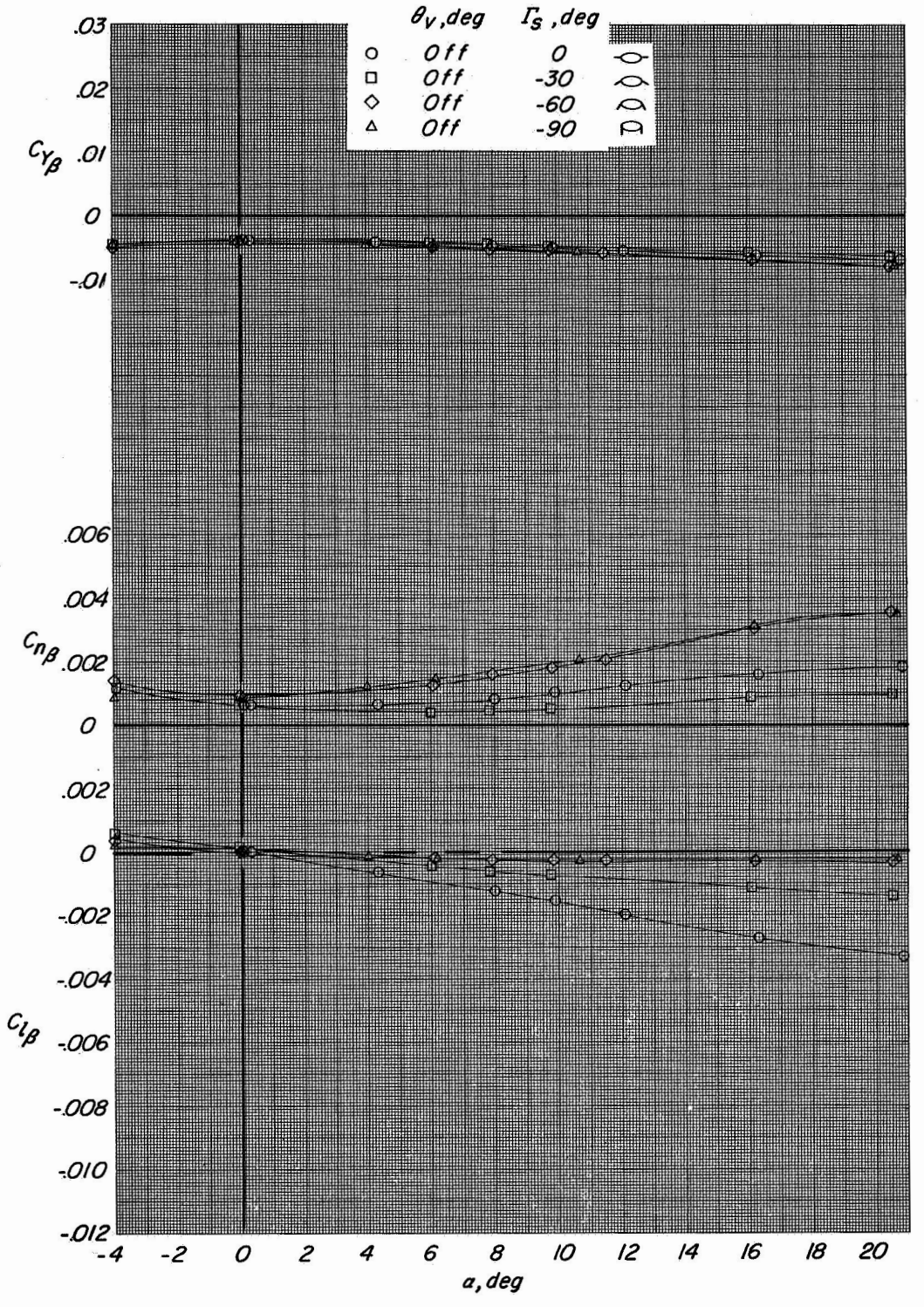

(b) Lateral-directional characteristics.

Figure 4.- Concluded.

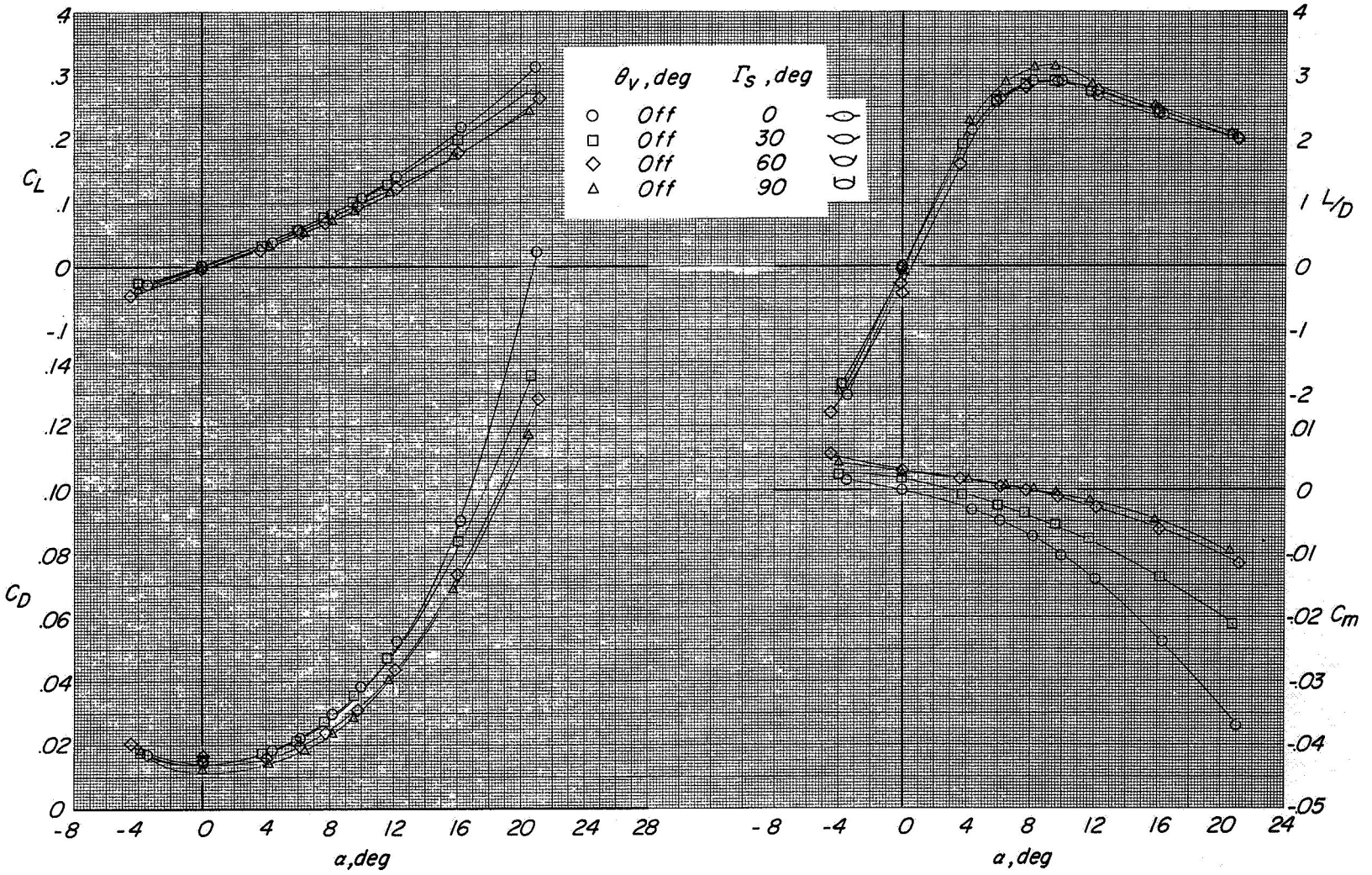

(a) Longitudinal characteristics.

Figure 5.- Effect of outboard stabilizers at positive dihedral angles on aerodynamic characteristics of f = 6.14 body.

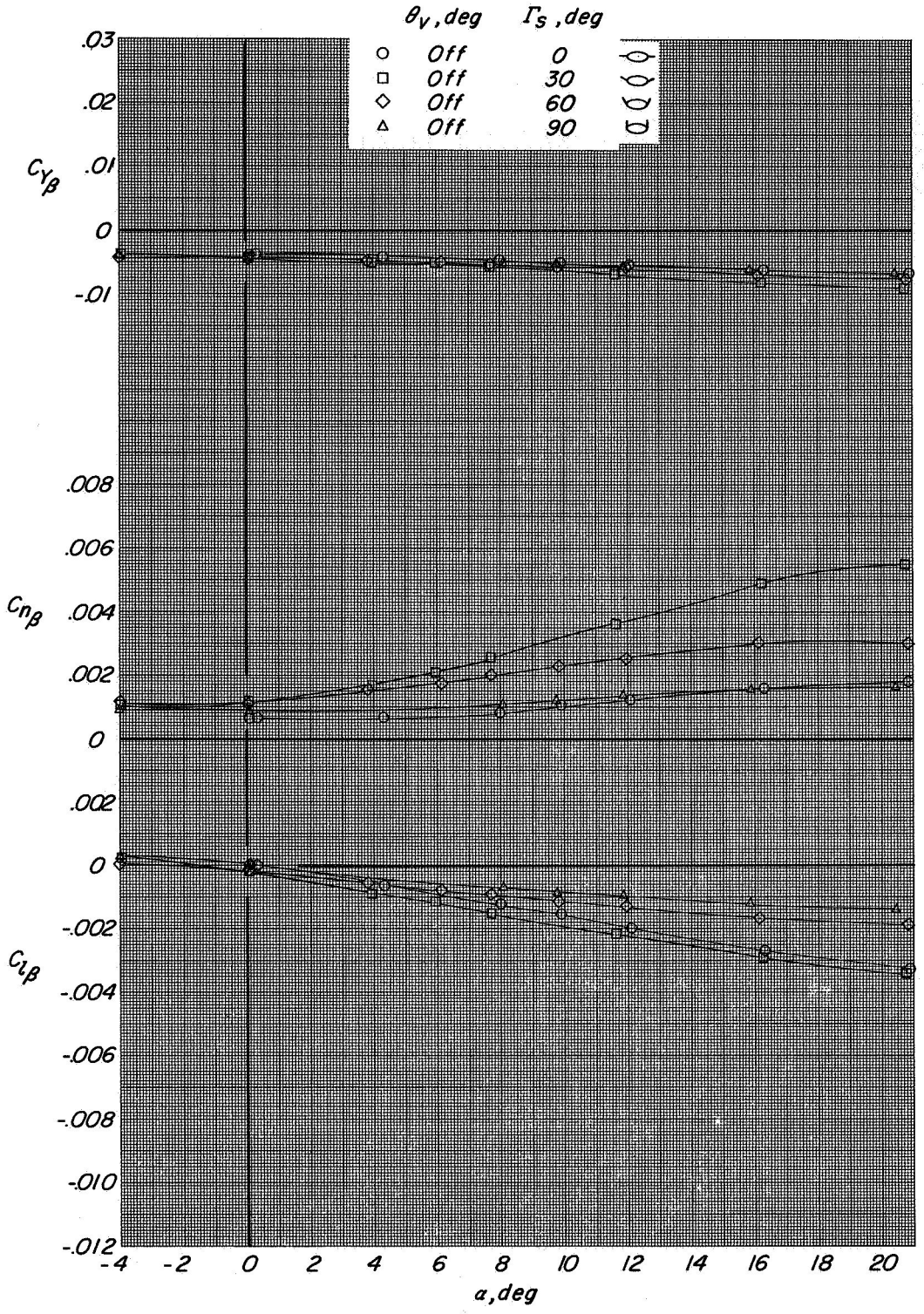

(b) Lateral-directional characteristics.

Figure 5.- Concluded.

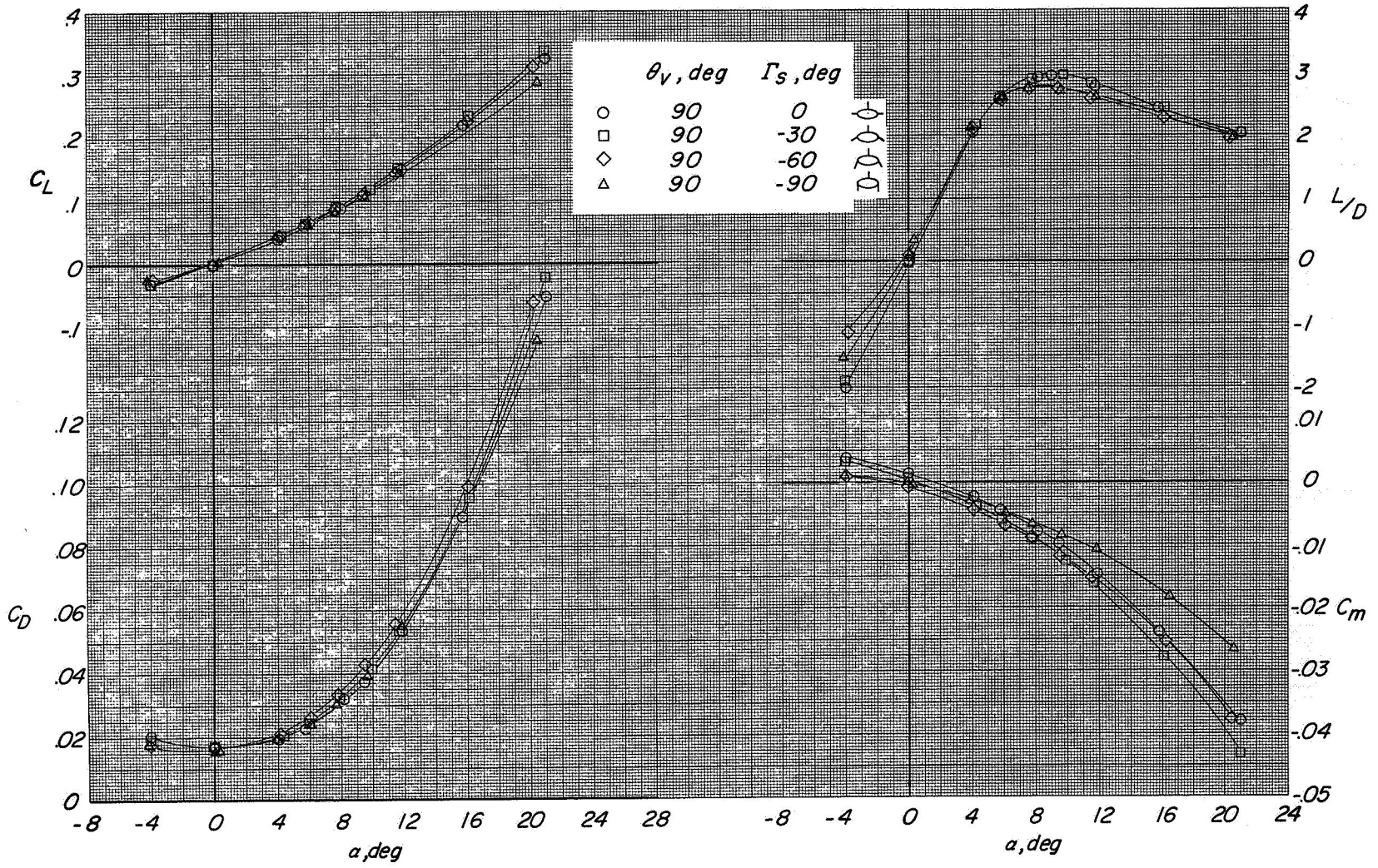

(a) Longitudinal characteristics.

Figure 6.- Effect of outboard stabilizers at negative dihedral angles on aerodynamic characteristics of f = 6.14 body and $\theta_V = 90^0$ configuration.

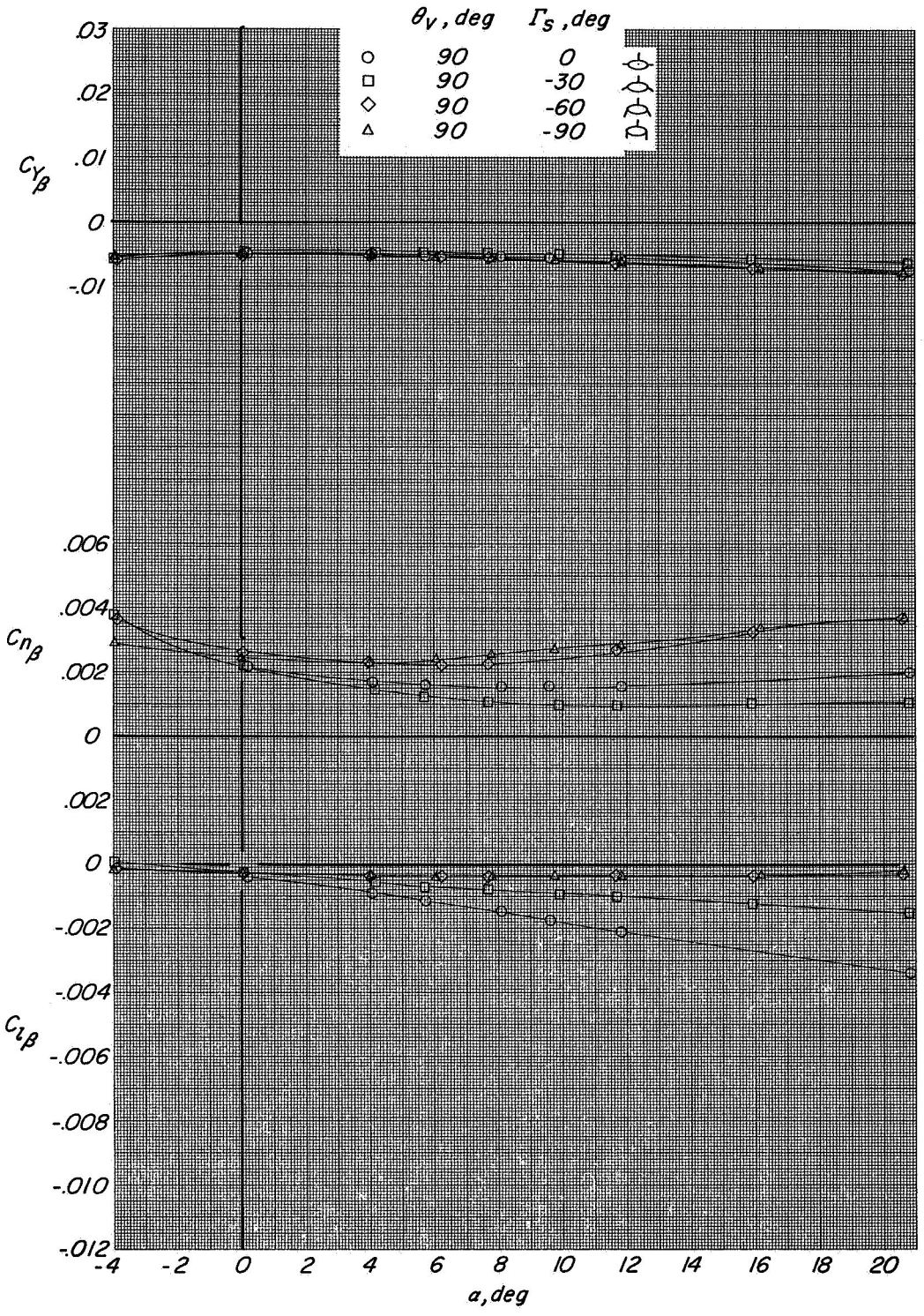

(b) Lateral-directional characteristics.

Figure 6.- Concluded.

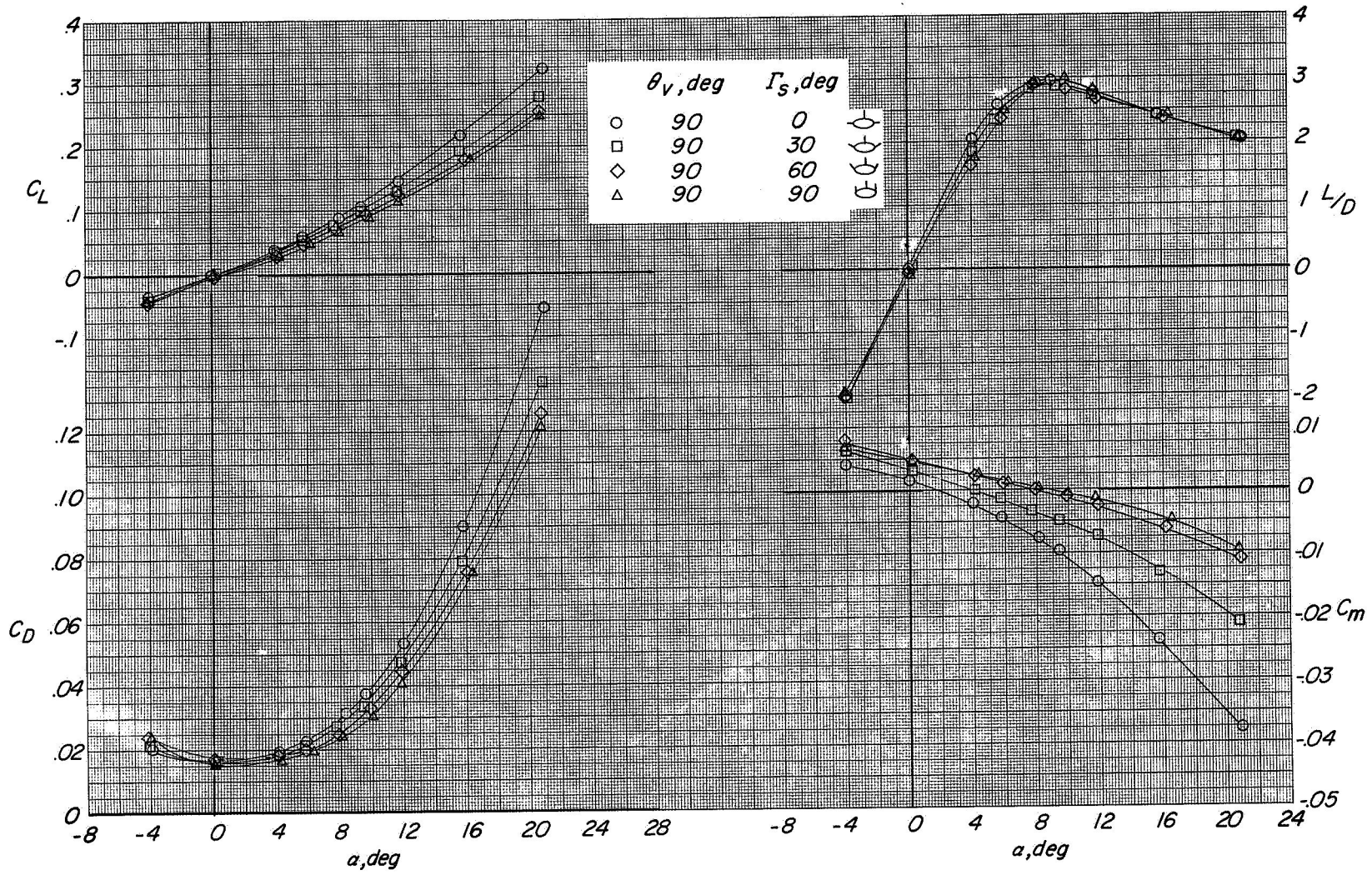

(a) Longitudinal characteristics.

Figure 7.- Effect of outboard stabilizers at positive dihedral angles on aerodynamic characteristics of f = 6.14 body and $\theta_V = 90^0$ configuration.

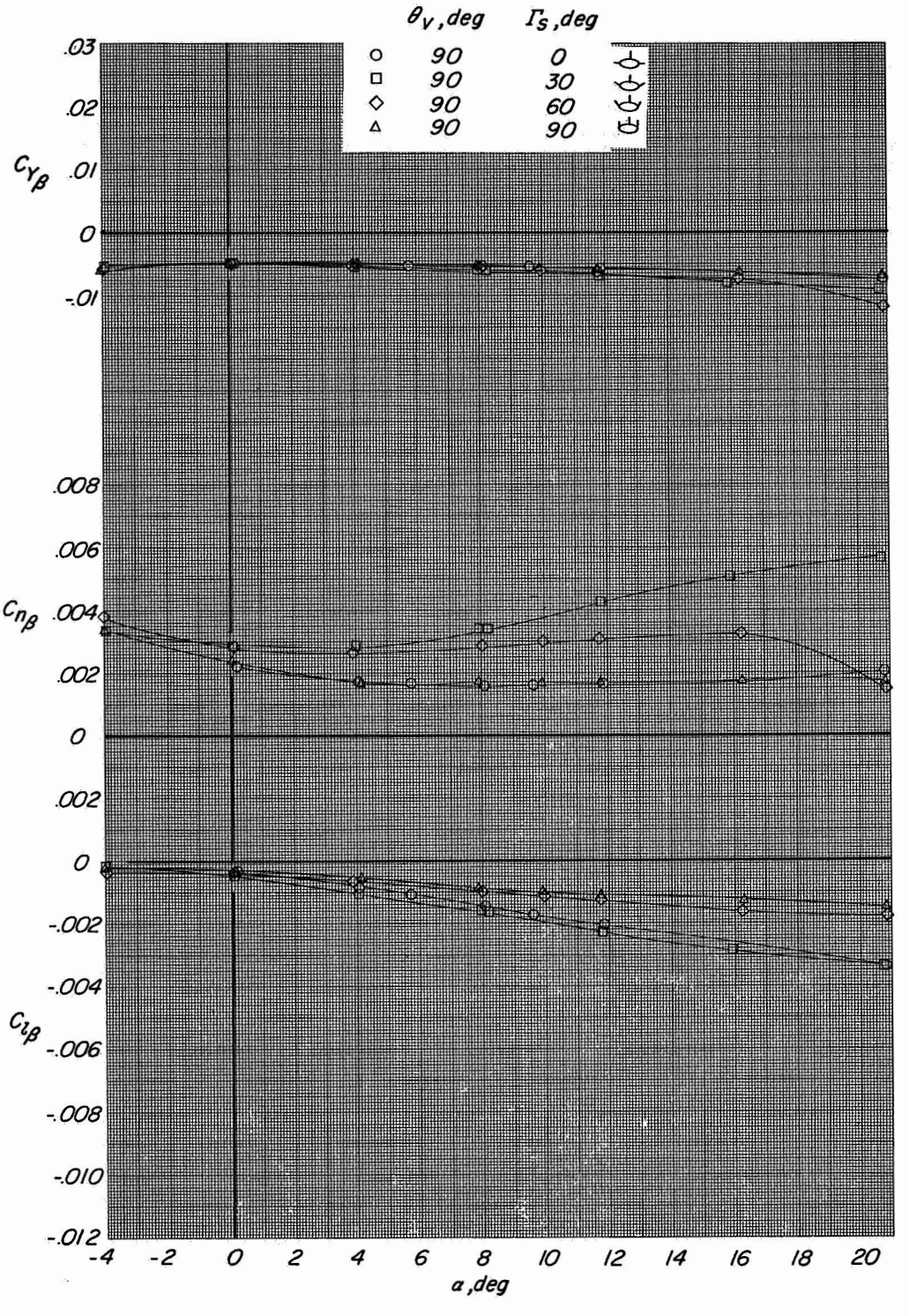

(b) Lateral-directional characteristics.

Figure 7.- Concluded.

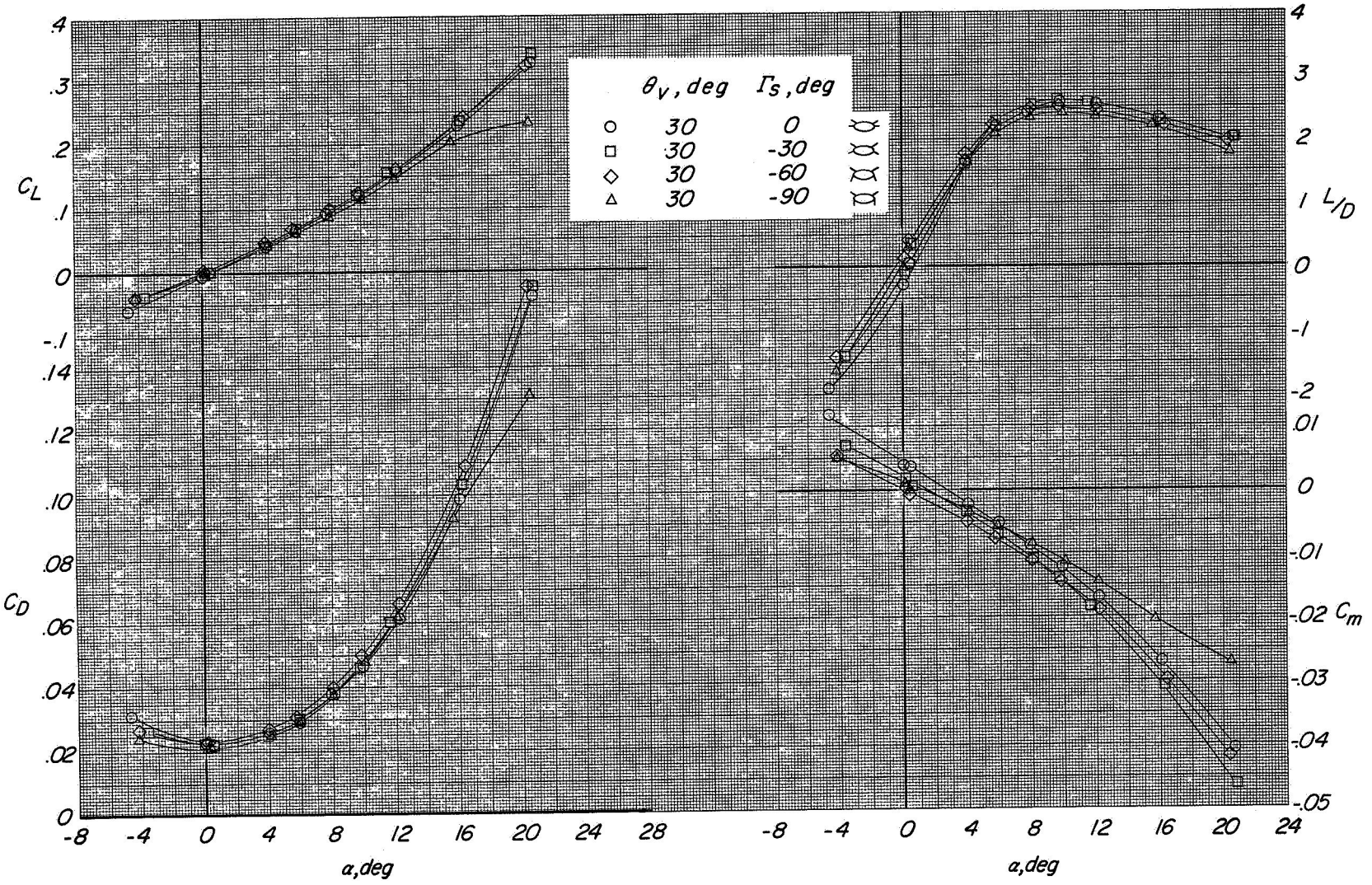

(a) Longitudinal characteristics.

Figure 8.- Effect of outboard stabilizers at negative dihedral angles on aerodynamic characteristics of f = 6.14 body and $\theta_V = 30^0$ configuration.

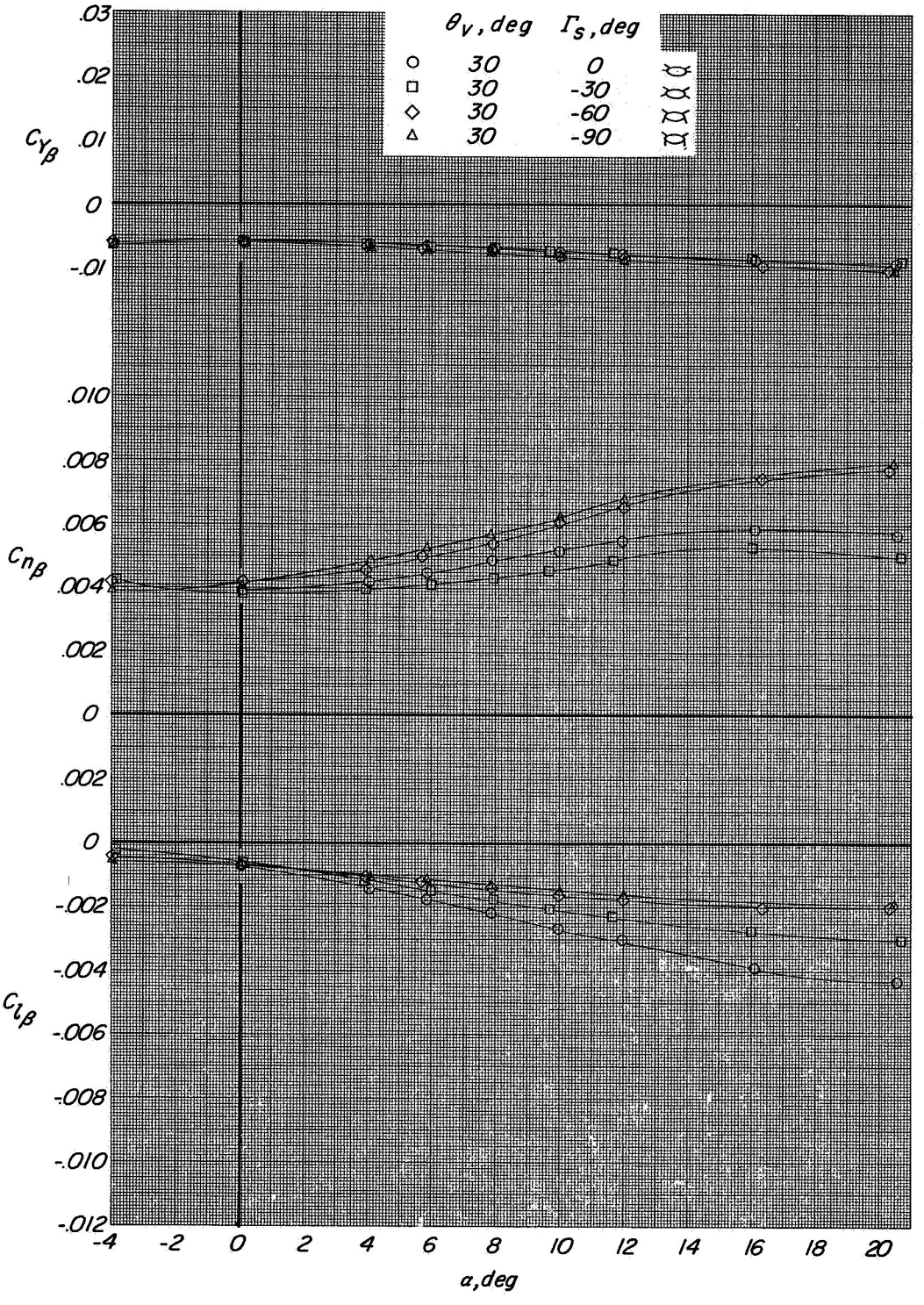

(b) Lateral-directional characteristics.

Figure 8.- Concluded.

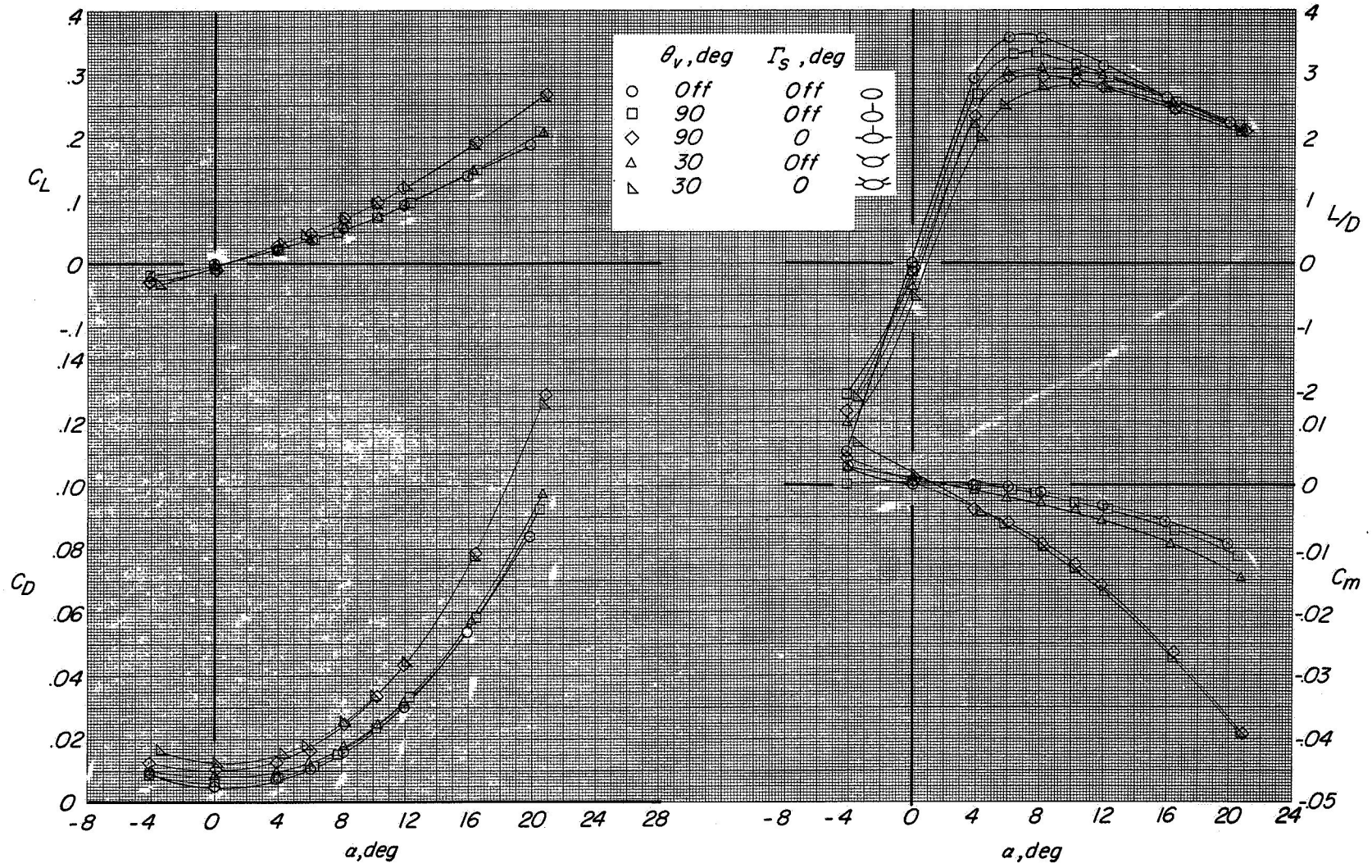

(a) Longitudinal characteristics.

Figure 9.- Effect of addition of tails and stabilizers on aerodynamic characteristics of f = 9.83 body.

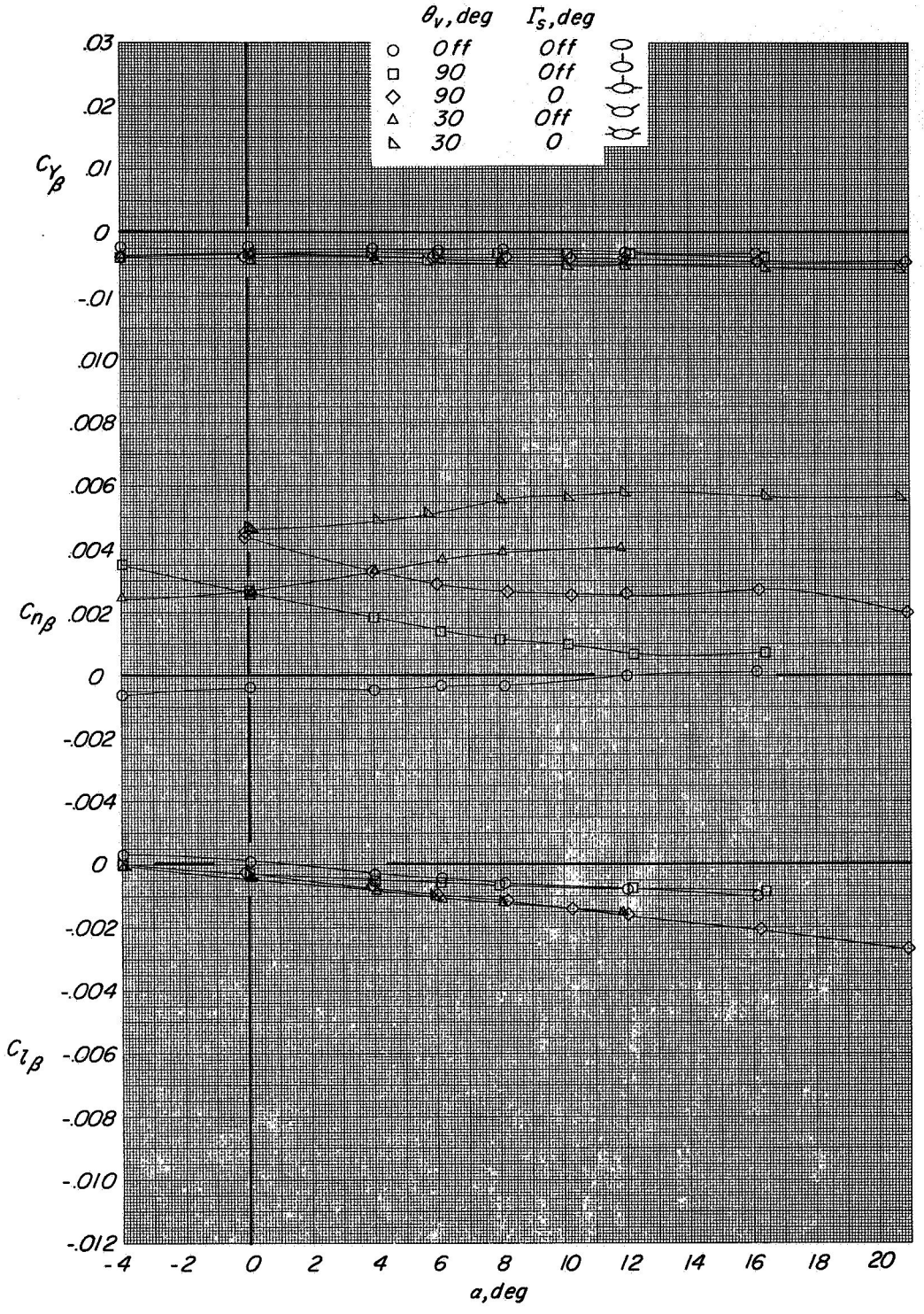

(b) Lateral-directional characteristics.

Figure 9.- Concluded.

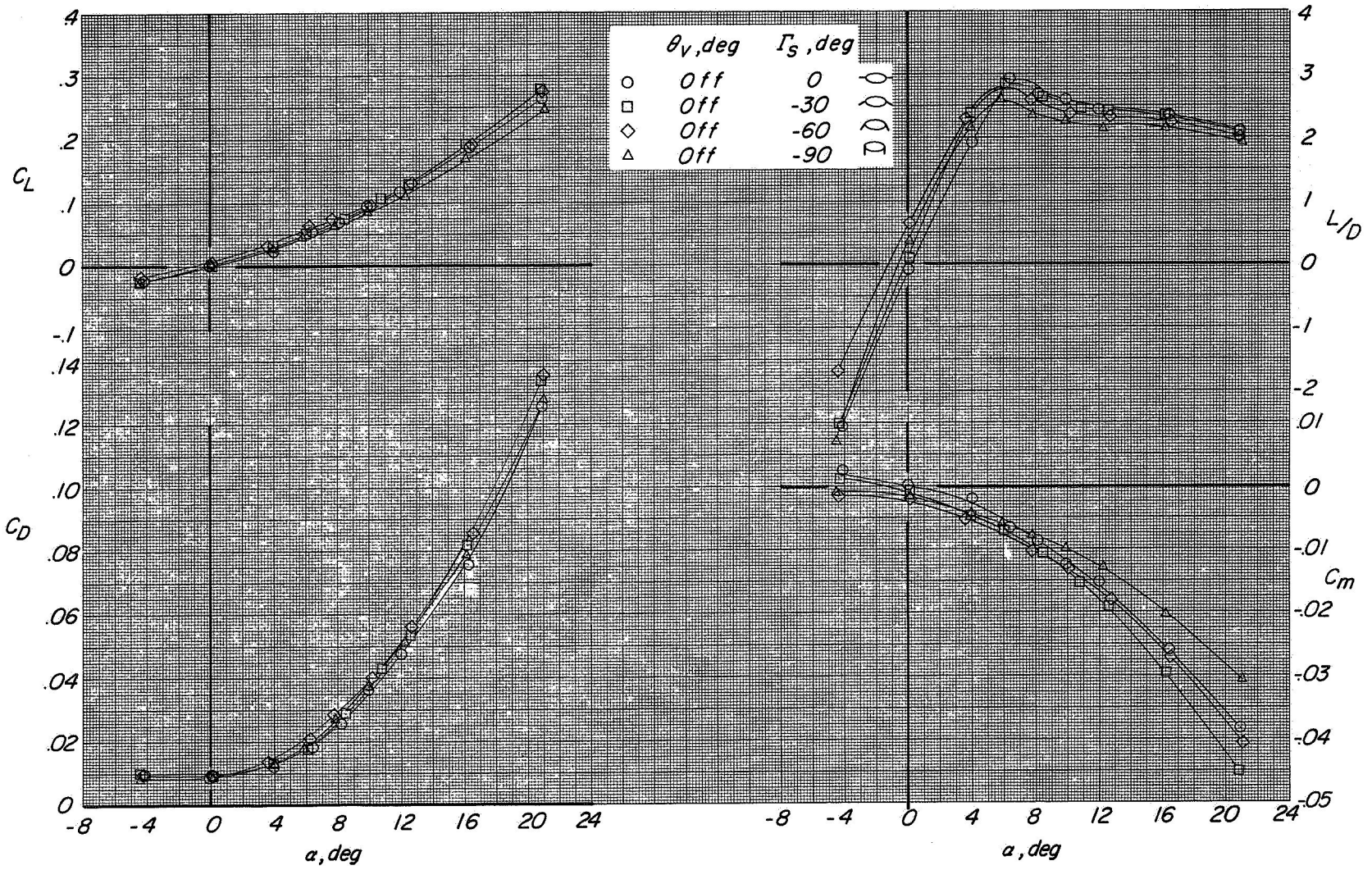

(a) Longitudinal characteristics.

Figure 10.- Effect of outboard stabilizers at negative dihedral angles on aerodynamic characteristics of f = 9.83 body.

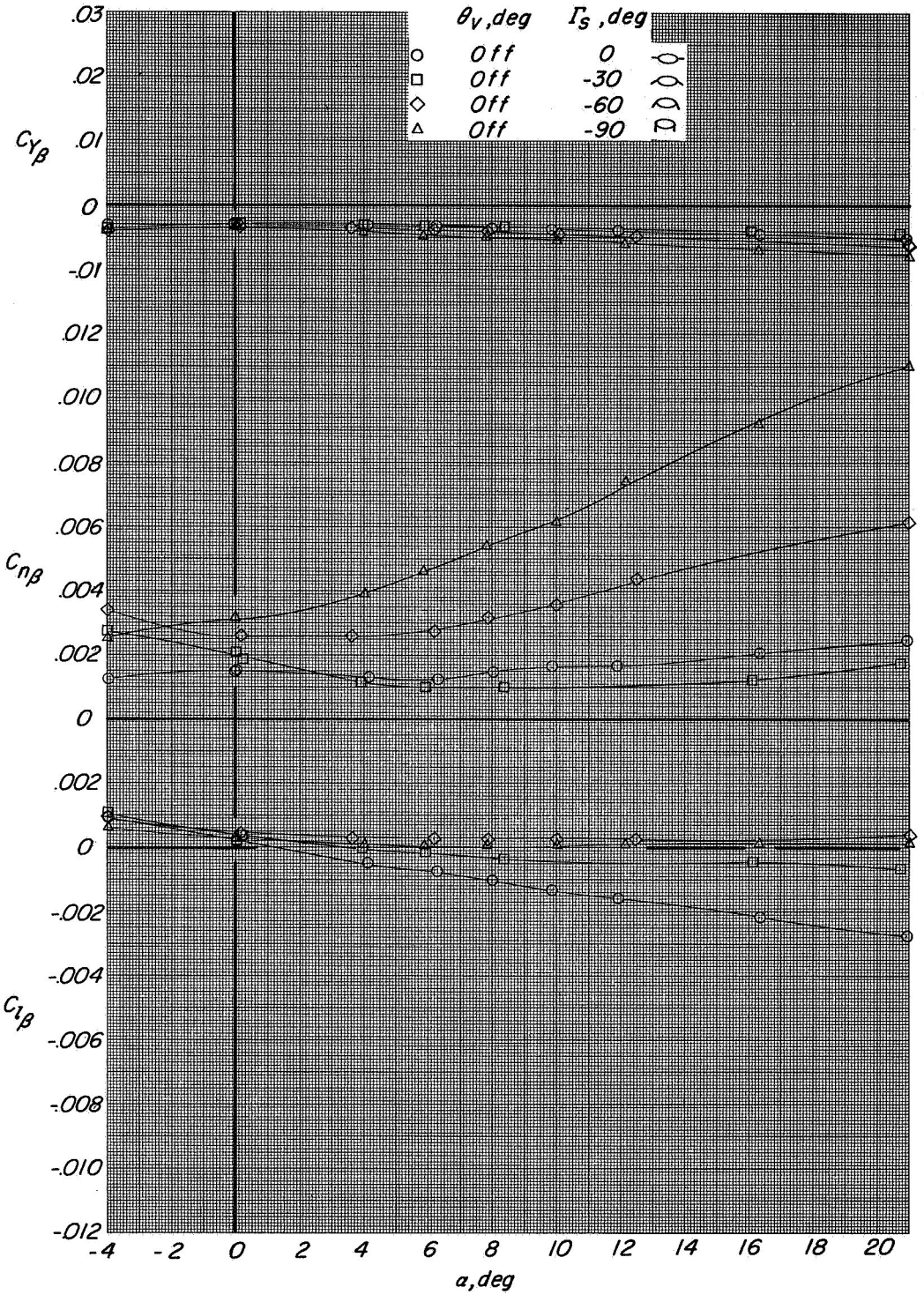

(b) Lateral-directional characteristics.

Figure 10.- Concluded.

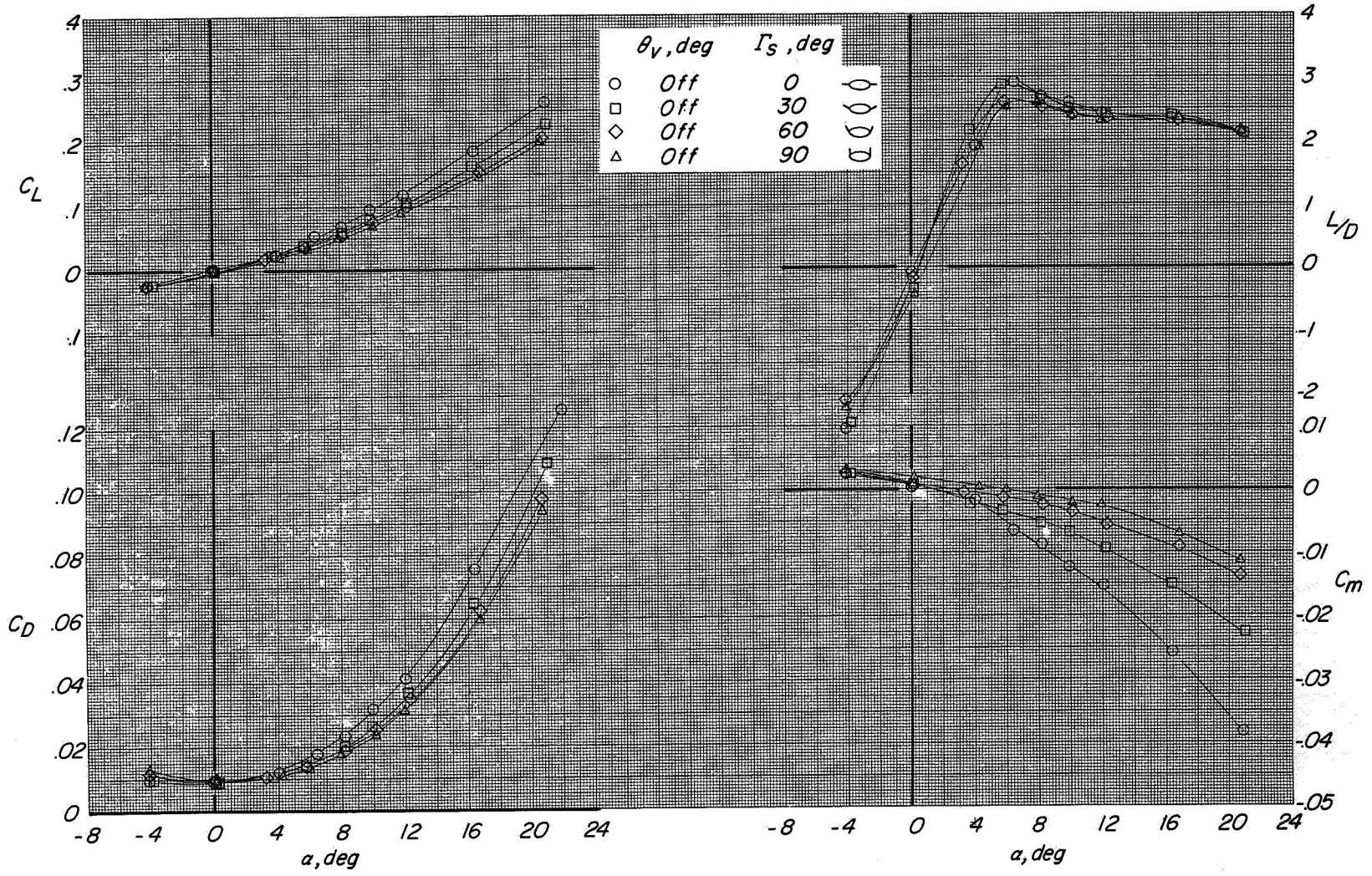

(a) Longitudinal characteristics.

Figure 11.- Effect of outboard stabilizers at positive dihedral angles on aerodynamic characteristics of f = 9.83 body.

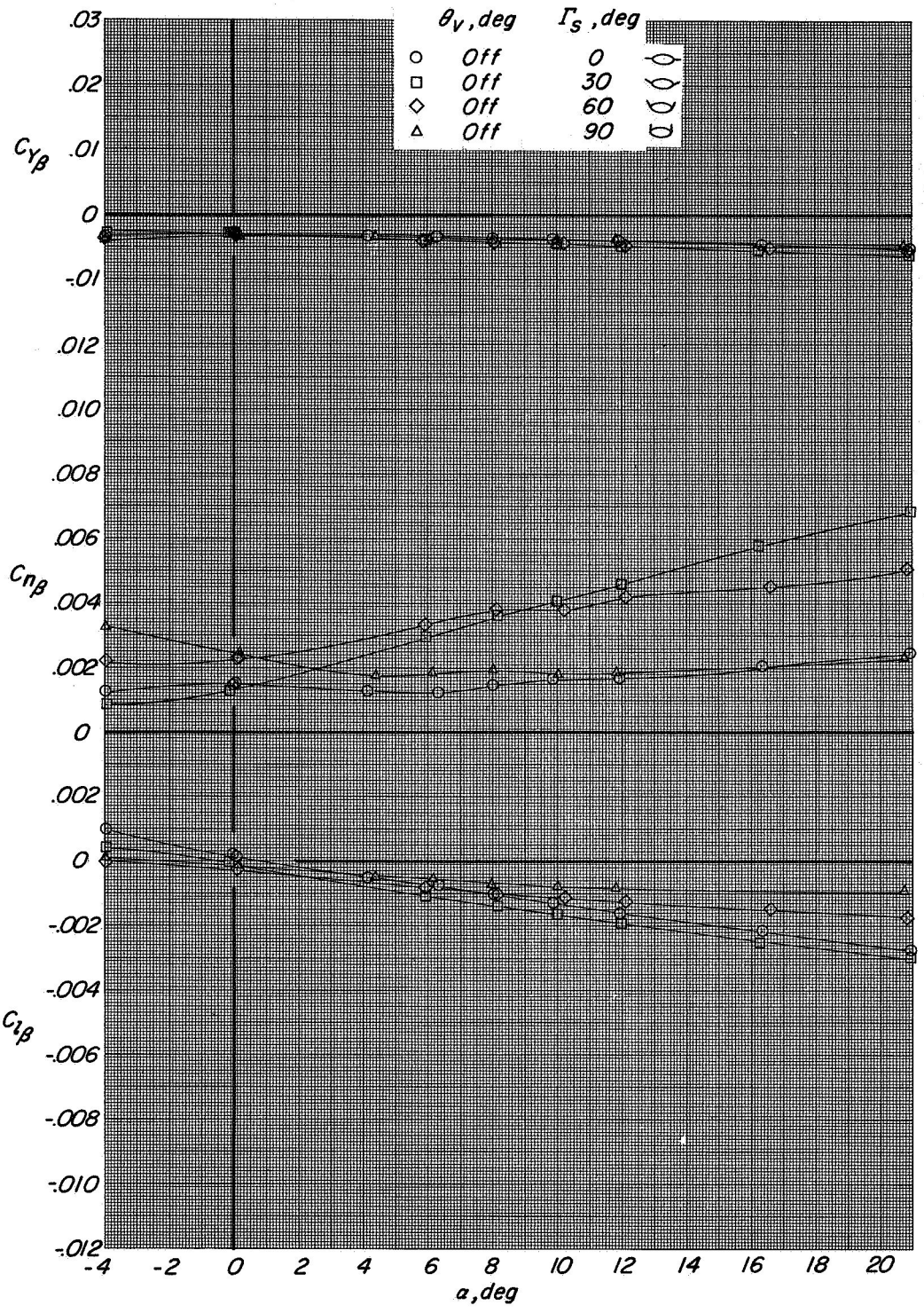

(b) Lateral-directional characteristics.

Figure 11.- Concluded.

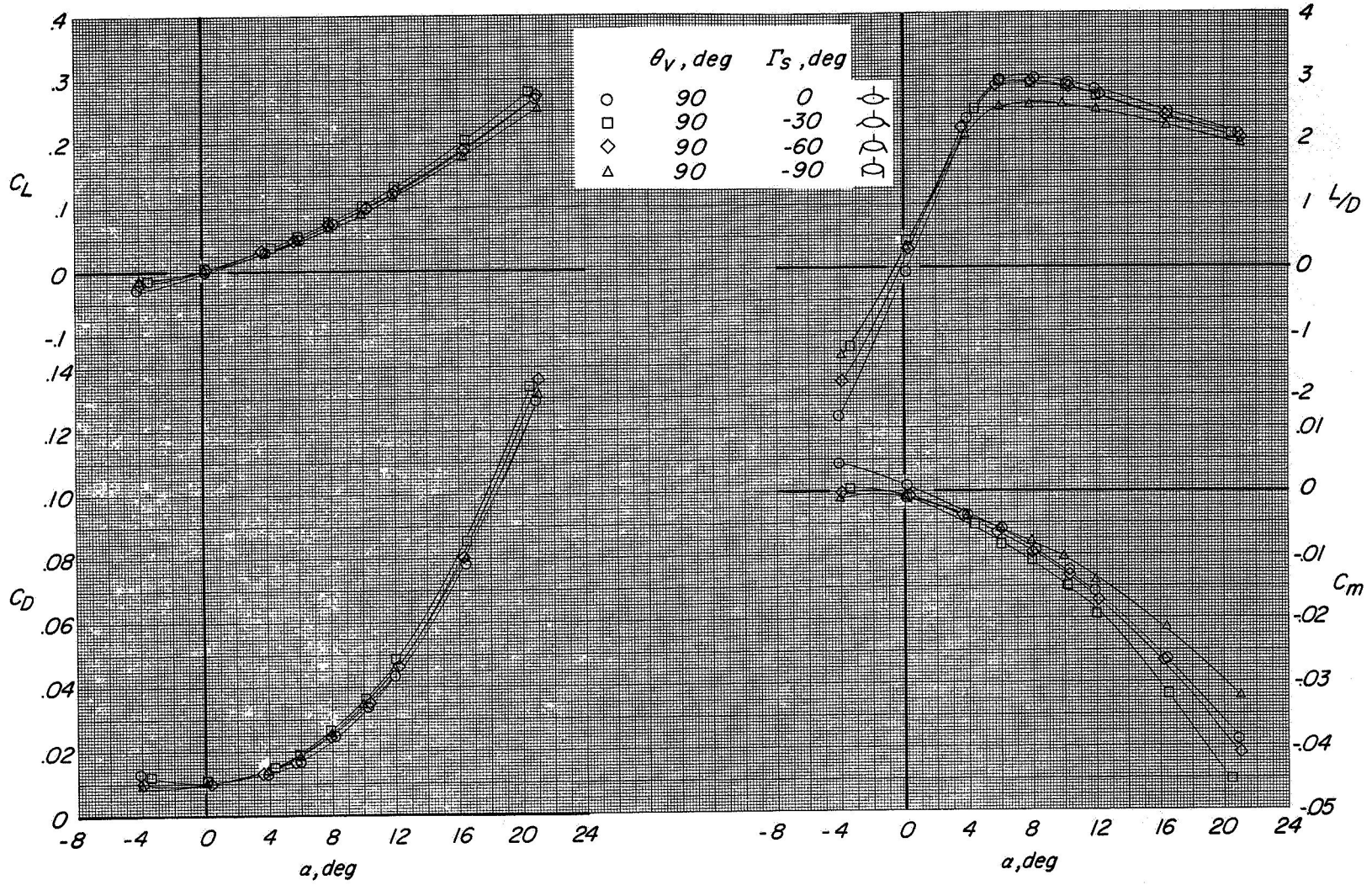

(a) Longitudinal characteristics.

Figure 12.- Effect of outboard stabilizers at negative dihedral angles on aerodynamic characteristics of f = 9.83 body and $\theta_V = 90^0$ configuration.

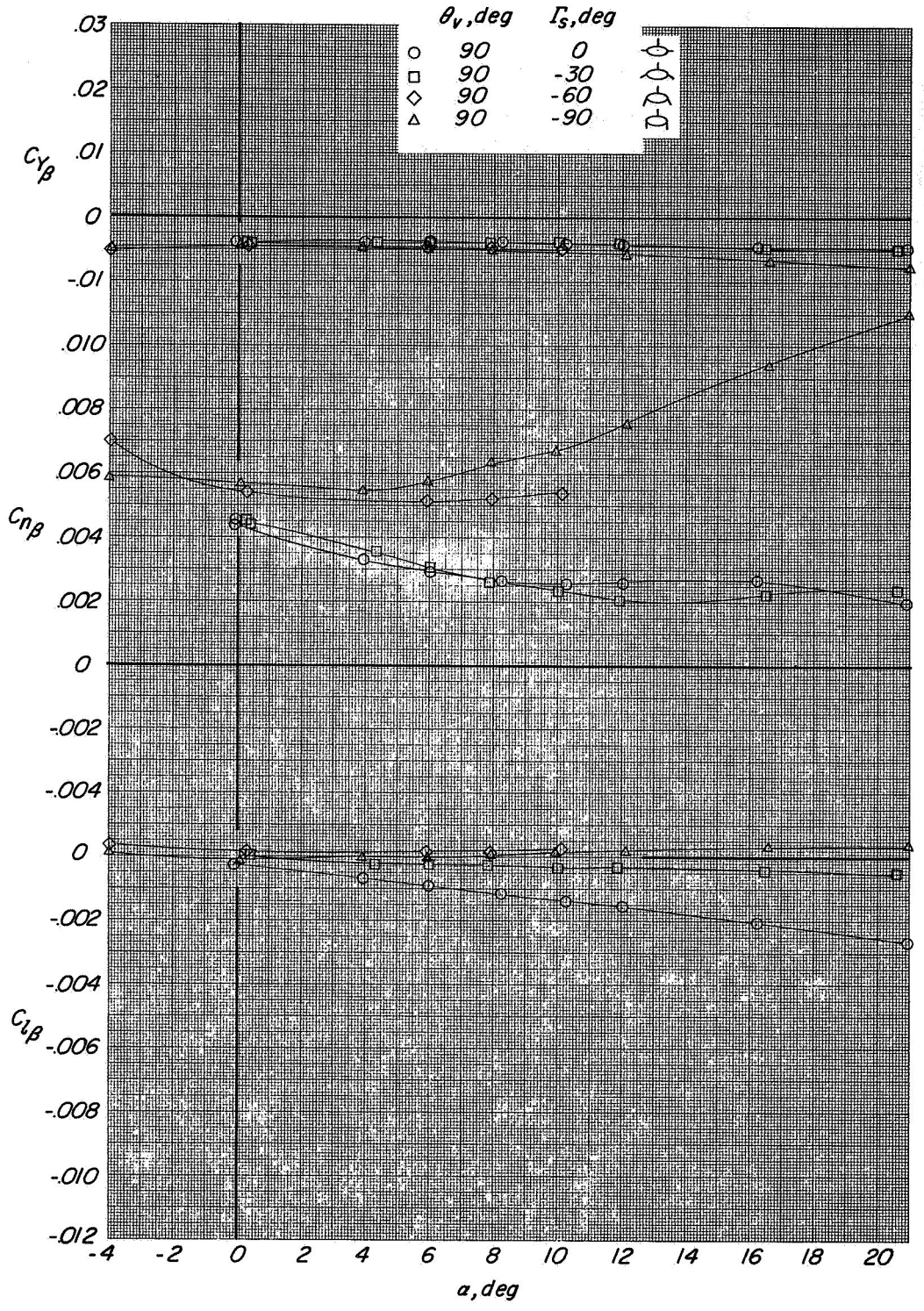

(b) Lateral-directional characteristics.

Figure 12.- Concluded.

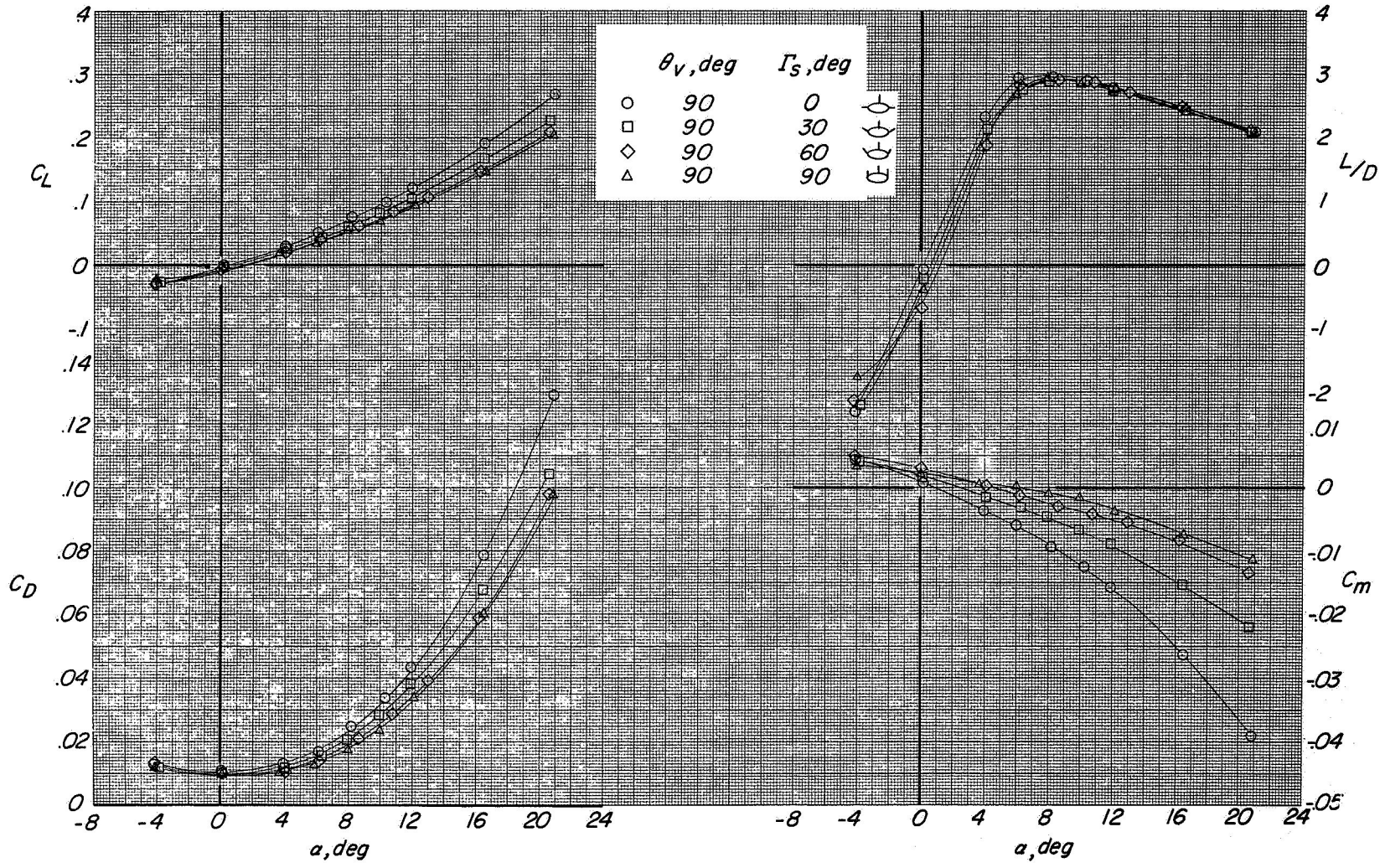

(a) Longitudinal characteristics.

Figure 13.- Effect of outboard stabilizers at positive dihedral angles on aerodynamic characteristics of f = 9.83 body and $\theta_V = 90^0$ configuration.

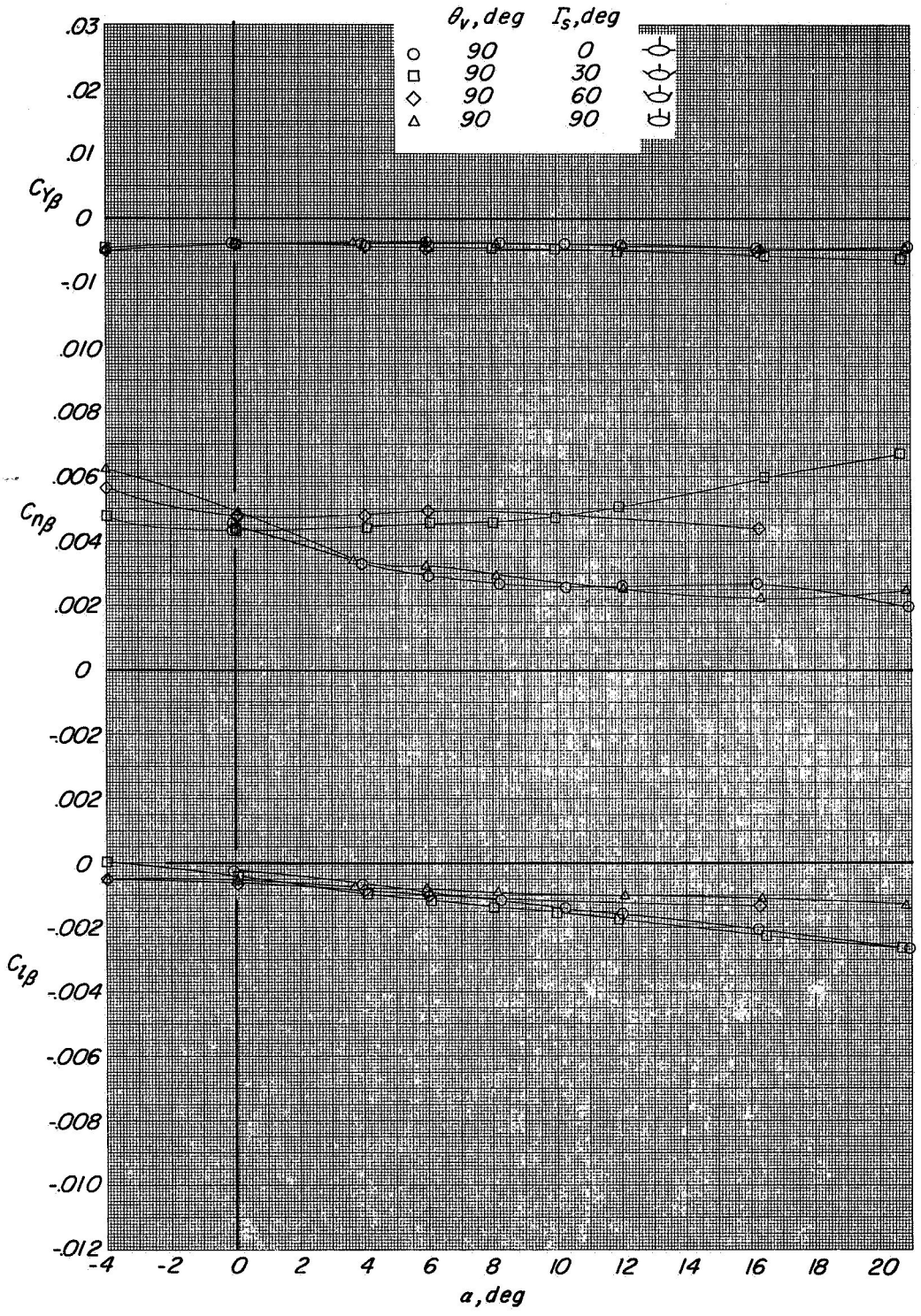

(b) Lateral-directional characteristics.

Figure 13.- Concluded.

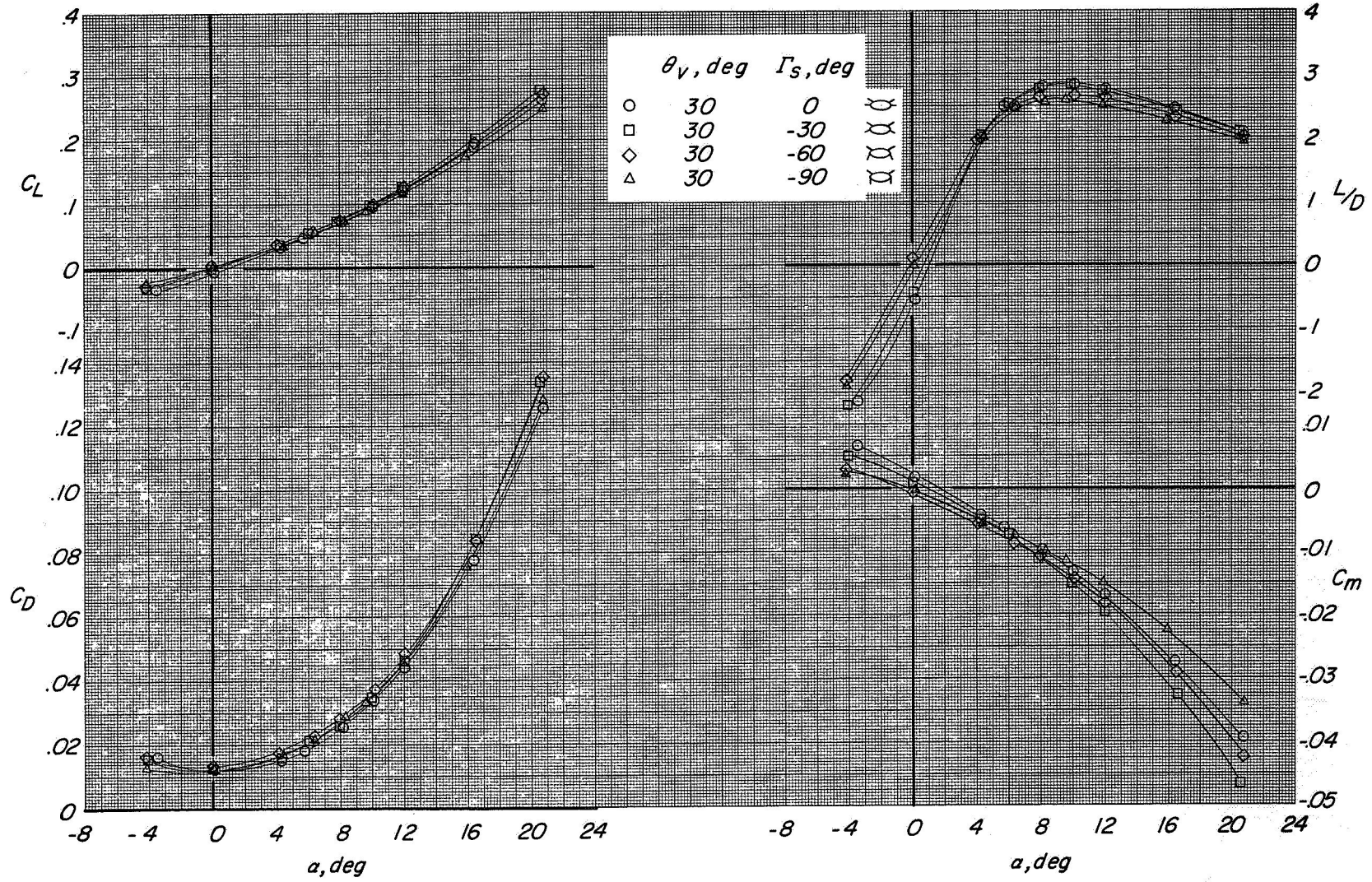

(a) Longitudinal characteristics.

Figure 14.- Effect of outboard stabilizers at negative dihedral angles on aerodynamic characteristics of f = 9.83 body and $\theta_V = 30^0$ configuration.

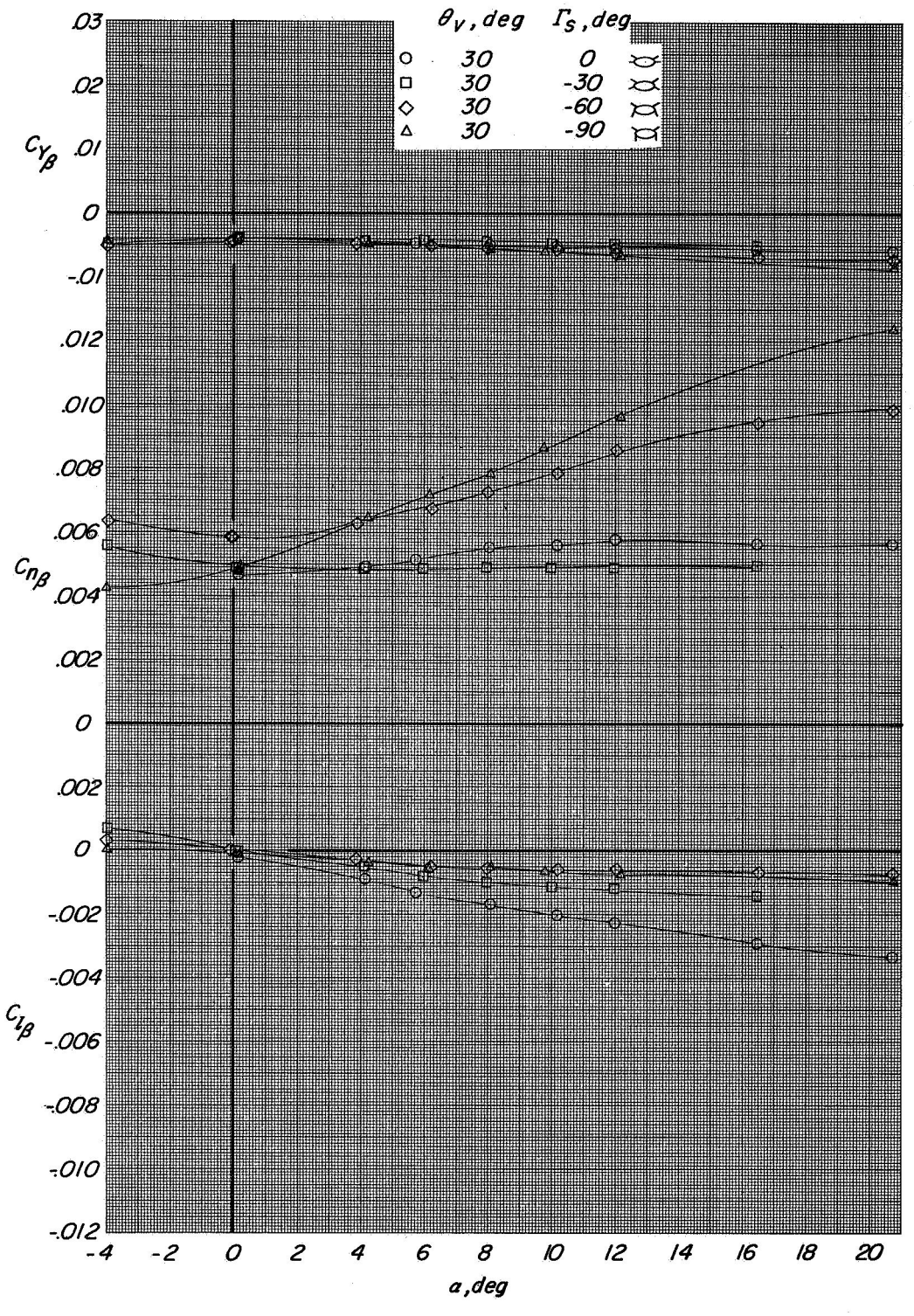

(b) Lateral-directional characteristics.

Figure 14.- Concluded.

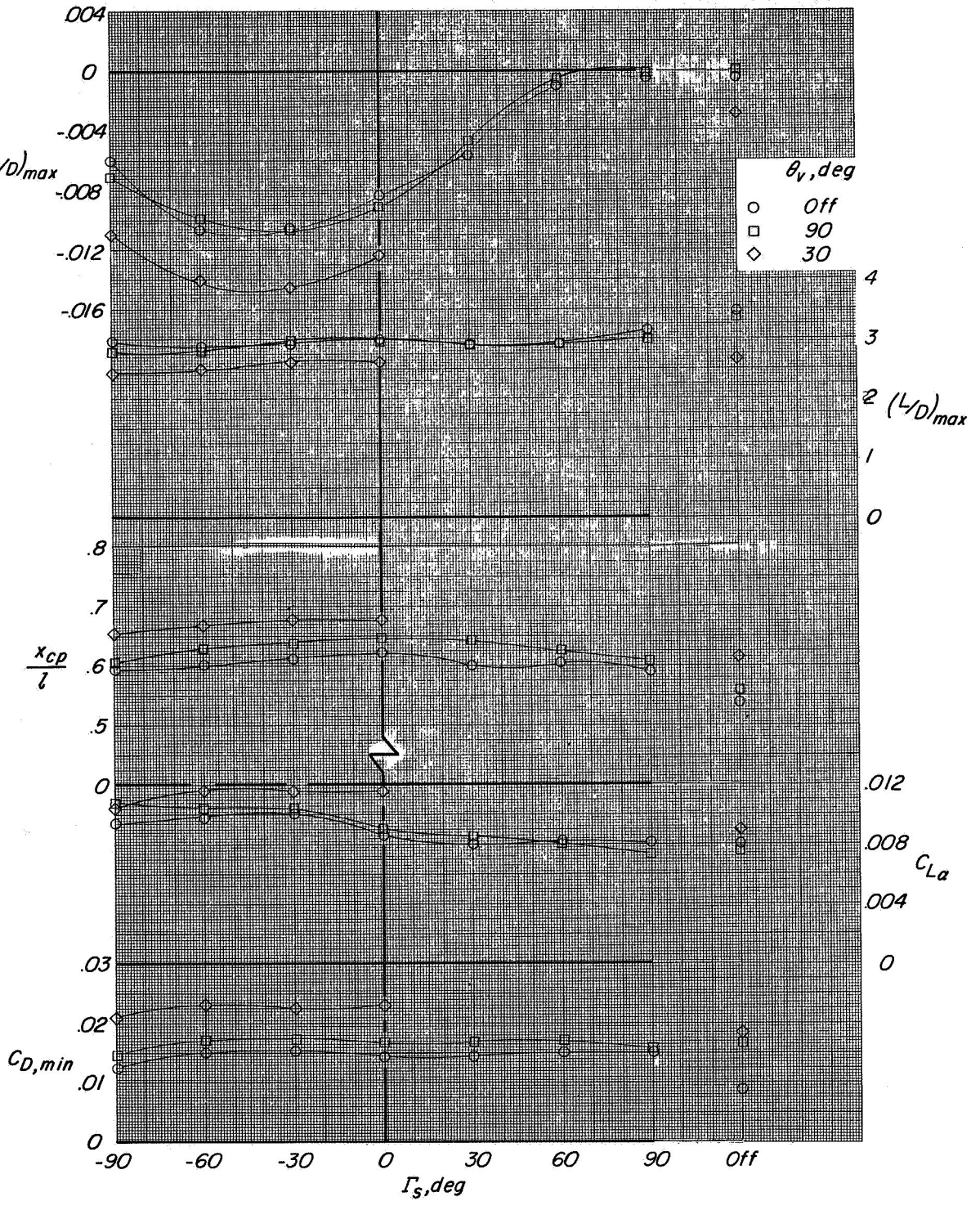

Figure 15.- Summary of the longitudinal aerodynamic characteristics for the f = 6.14 body.

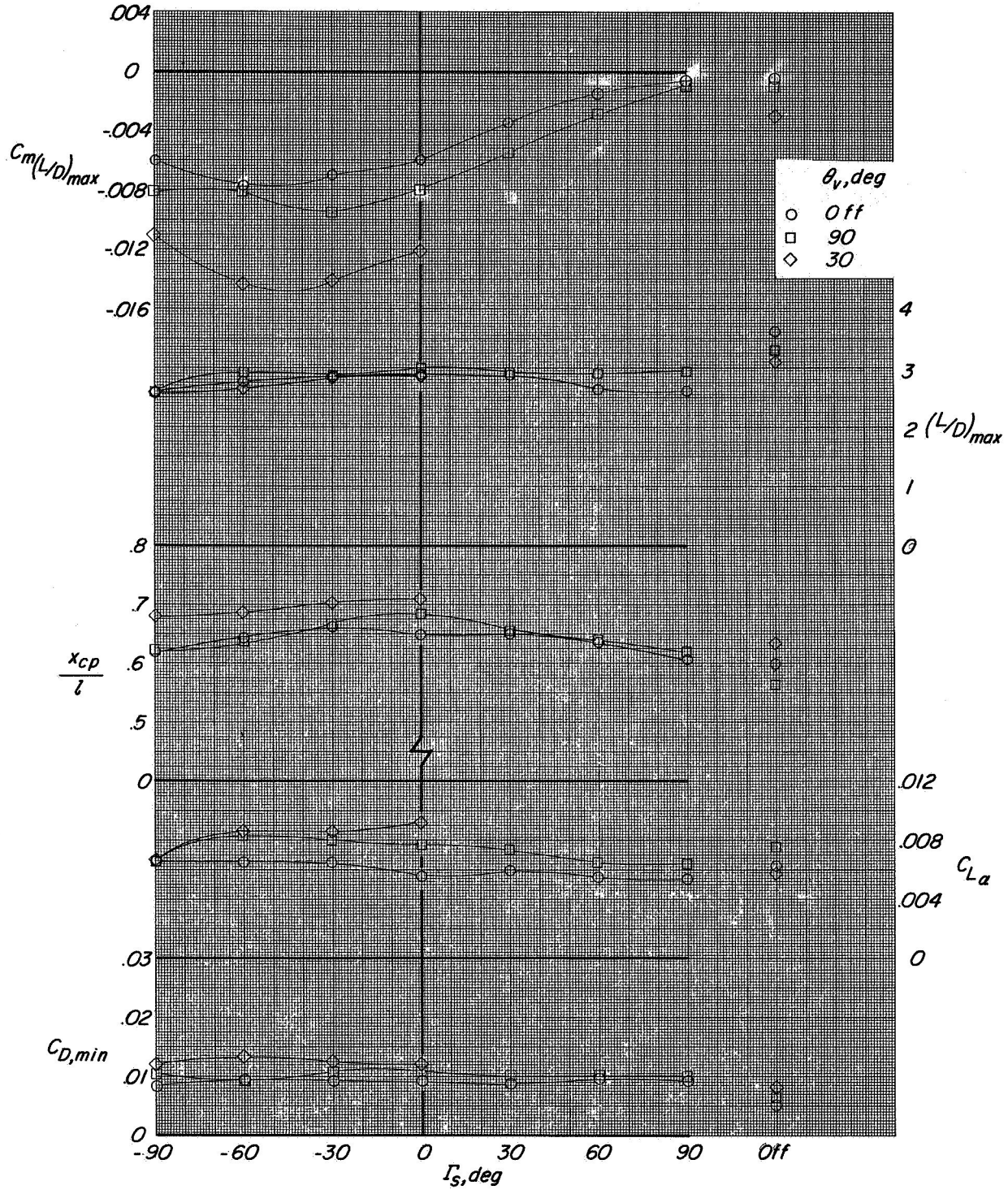

Figure 16.- Summary of the longitudinal aerodynamic characteristics for the f = 9.83 body.

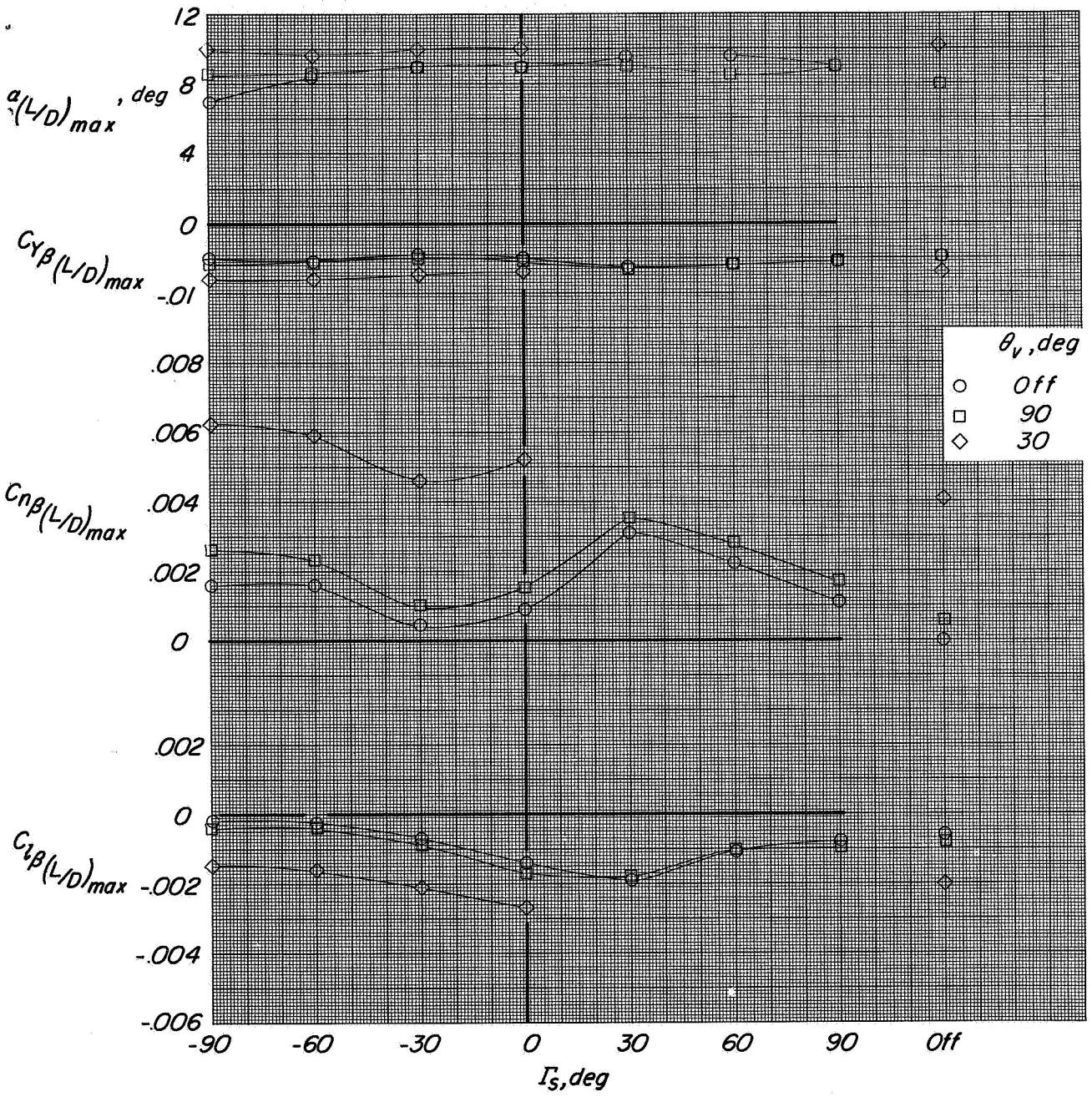

Figure 17.- Summary of the lateral-directional stability characteristics at $(L/D)_{max}$ for the f = 6.14 body.

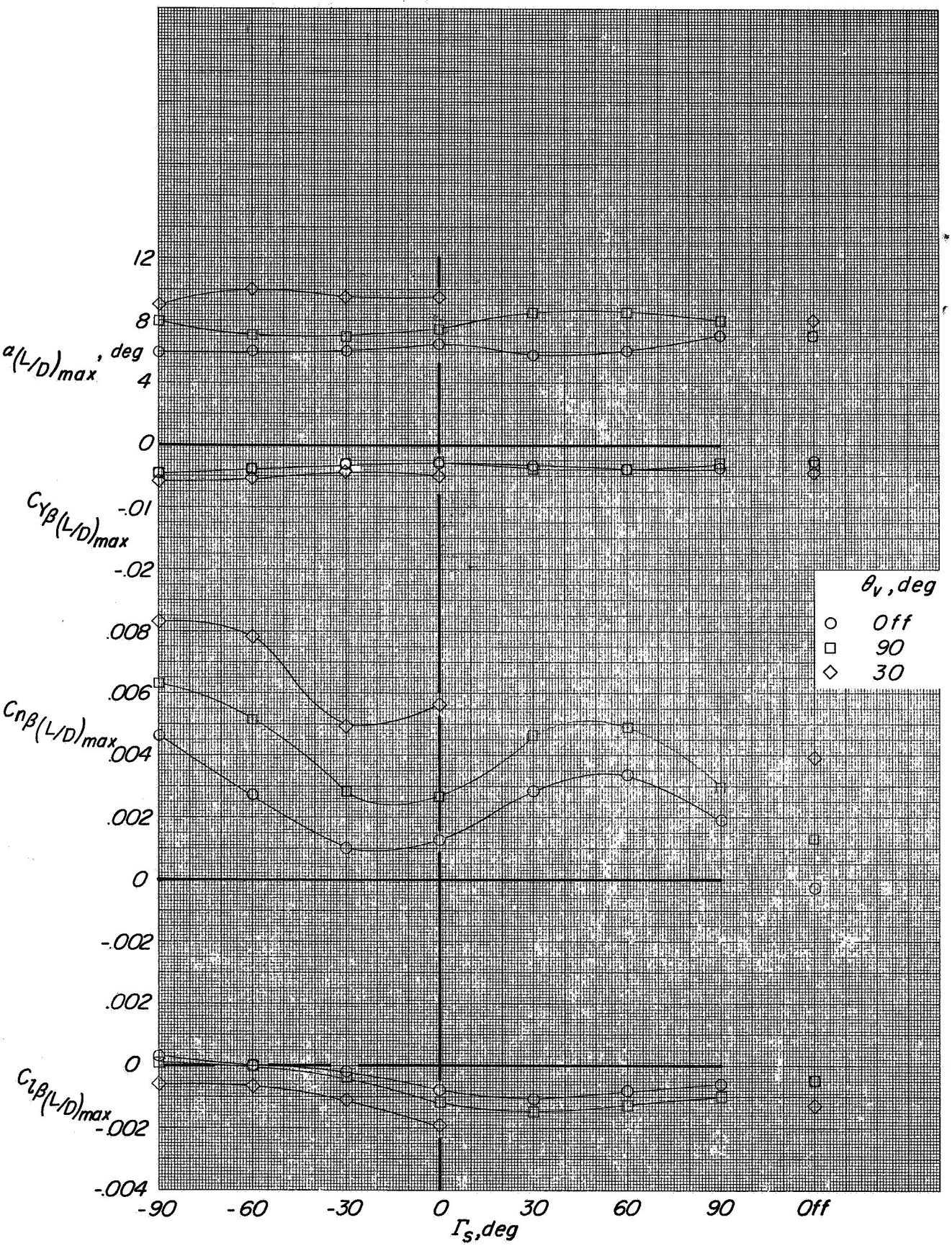

Figure 18.- Summary of the lateral-directional stability characteristics at $(L/D)_{max}$ for the f = 9.83 body.

NASA-Langley, 1968 — 1 L-5853